DOKUZ EYLÜL UNIVERSITY
GRADUATE SCHOOL OF NATURAL AND APPLIED SCIENCES

ENVIRONMENTAL EFFECTS ON PIN-LOADED LAMINATED COMPOSITES

by
Halit KANLIOĞLU

June, 2009
İZMİR

ENVIRONMENTAL EFFECTS ON PIN-LOADED LAMINATED COMPOSITES

A Thesis Submitted to the
Graduate School and Applied Sciences of Dokuz Eylül University
In Partial Fulfillment of the Requirements for the
Degree of Master of Science in
Mechanical Engineering, Mechanics Program

by
Halit KANLIOĞLU

June, 2009
İZMİR

M.Sc THESIS EXAMINATION RESULT FORM

We have read the thesis entitled **"ENVIRONMENTAL EFFECTS ON PIN-LOADED LAMINATED COMPOSITES"** completed by **HALİT KANLIOĞLU** under supervision of **PROF. DR. RAMAZAN KARAKUZU** and we certify that in our opinion it is fully adequate, in scope and in quality, as a thesis for the degree of Master of Science.

Prof. Dr. Ramazan KARAKUZU

Supervisor

Doç. Dr. İsmail ÖZDEMİR

(Jury Member)

Doç. Dr. Cesim ATAŞ

(Jury Member)

Prof.Dr. Cahit HELVACI
Director
Graduate School of Natural and Applied Sciences

ACKNOWLEDGEMENTS

With all my heart first and foremost, deep gratitude and appreciation goes to my supervisor, Professor Dr. Ramazan KARAKUZU, for his help, excellent guidance and continuous encouragement throughout this work.

I would like to thank all my co workers in the Composite Research Laboratory and Mechanical Test and Research Laboratory. In particular, I would like to thank Research Assistant Mehmet Emin DENİZ, Dr. Bülent Murat İÇTEN, Assoc. Professor Dr. Cesim ATAS and Research Assistant Semih BENLİ.

Finally I wish to express sincere thanks to magnificent peoples who are my parents, my sister and my fiance Leyla ÖZGÜR for their moral support, tolerance and understanding while preparing this thesis. Without their help and love, the completion of this dissertation is impossible. For this reason, this dissertation is dedicated to them.

Halit KANLIOĞLU

ENVIRONMENTAL EFFECTS ON PIN-LOADED LAMINATED COMPOSITES

ABSTRACT

The aim of this study was to study the effect of the sea water on the bearing strength behavior of the glass-epoxy laminated composite. The ratio of the edge distance to the pin diameter, and the ratio of the specimen width to the pin diameter (W/D) were systematically varied during experiments. The ratio of the edge distance to the pin diameter were changed from one to five and the ratio of the specimen width to the pin diameter were selected as three and four for this study. The hole of the plate is subjected to a traction force by a pin.

For this study, layered composite materials were manufactured, at İzoreel firm, at one hundred and twenty degree Celsius and under two hundred and fifty kilo Pascal pressure. Two different stacking sequences were choosen. One of them was produced at zero degrees orientation angle of fiber to obtain the mechanical properties of the laminated composite material. The mechanical properties of the laminated composite material were obtained from standard tests by absorping natural water and sea water. Second one was of stacking sequence zero degrees and ninety degrees multiply three with the symmetric of them to investigate the effects of sea water on the bearing strength behavior of the laminated composite.

Failure modes and maximum failure loads of the specimens are found in experimental study. Experimental study includes one, three, six and nine month periods for absorption of sea water into glass fiber-epoxy composites. So the specimens kept into sea water one, three, six, and nine month periods. For every period, failure modes and maximum failure loads of the specimens are found in experimental study.

Keywords: Composite plates, Failure analysis, Failure modes, Bearing strength.

ÇEVRE KOŞULLARININ PİM BAĞLANTILI KOMPOZİT PLAKLARIN HASAR DAVRANIŞINA ETKİSİ

ÖZ

Bu çalışmanın hedefi deniz suyunun cam epoksi dokunmuş tabakalı kompozitlerin yatak gerilme davranışları üzerindeki etkilerini incelemektir. Numunenin uç kısmının deliğin çapına oranı ve genişliğinin deliğin çapına oranı deneyler süresince sistematik olarak değiştirilmiştir. Bu çalışmada numunenin uç kısmının deliğin çapına oranı birden beşe kadar, genişliğinin deliğin çapına oranı ise üç ve dört olarak seçildi. Numune plakanın deliği bir pim yardımıyla değişken yayılı yüke mağruz bırakılmıştır.

Bu çalışma için tabakalı kompozit malzeme İzoreel firmasında yüzyirmi Santigrat derece ve iki yüz elli kilo Pascal basınç altında üretilmiştir. İki farklı dizi yığılım seçilmiştir. Bunlardan biri tabakalı kompozit malzemenin mekanik özelliklerinin belirlenmesi için sıfır derece oryantasyon açılı olarak üretilmiştir. Tabakalı kompozit malzemenin mekanik özellikleri normal su ve deniz suyu emdirilerek standart testler neticesinde belirlenmiştir. İkincisi ise deniz suyunun tabakalı kompozitler üzerindeki yatak gerilme davranışının incelenmesi için üç adet sıfır ve doksan derece ile bunların simetriği oryantasyonlu olarak üretilmiştir.

Numunelerin hasar tipleri ve maksimum hasar yükleri deneysel olarak bulunmuştur. Deneysel çalışma cam lifi-epoksi kompozitin içerisine deniz suyunu emmesi için bir, üç, altı ve dokuz aylık süreleri içerir. Bu nedenle numuneler bir, üç, altı ve dokuz aylık süreler boyunca deniz suyu içerisinde tutulmuştur. Her periyot için hasar tipleri ve maksimum hasar yükleri bulunmuştur.

Anahtar sözcükler: Kompozit plakalar, Hasar analizi, Hasar tipleri, Yatak mukavemeti.

CONTENTS

Page

CHAPTER ONE
INTRODUCTION

1.1 Overview

There has been a growing interest, particularly in the few last decades, in the use of composite materials in structural applications ranging from aircraft and space structures to automotive and marine applications.

Glass-fibre reinforced polymer composites are often used in marine craft such as canoes, fishing trawlers, patrol boats and naval minehunting ships and in the non-pressure hull casing, sonar dome and masts of submarines. Fibreglass composites are also used in offshore drilling platforms for deck grates, low-pressure pipes and storage tanks, and in civil infrastructure for the repair, strengthening and rehabilitation of ageing pylons to bridges and piers.

When the boats built in recent years are compared to the boats of former years; it can be seen that the hull structures are produced to meet the demands related to higher loads; no matter whether the boat is a motorboat or a sailing yacht. This can be attributed to the competitive attitude of people: boat owners driving motorboats favor ever-faster boats, installing more powerful engines. On the other hand, owners of sail yachts favor larger sail areas, stainless steel rigging, synthetic sail fabrics, shorter fin keels, etc., even though the waves and wind have not changed for millennia. These preferences have resulted in increased stresses on hull material. Therefore, the designer has to deal with a higher structural loads and/or increasingly lighter structures. More accurate calculations are made with smaller margins of error or smaller factors of safety. What has made those lighter structures available is the use of advanced composite materials technology.

1.2 Objectives of the Present Study

Due to their high specific strength and specific stiffness, composite materials and thus composite joints are finding increasing application in a variety of engineering structures.

Joints are necessary load transfer elements of components or structures and the performance of these structures or components is critically dependent upon the behavior of any joints they contain. Joining by mechanical fasteners is a common practice in the assembly of structures and since joint failure can lead to premature failure of the structure, joint strength is an important property in any design. Mechanical joining requires rivets and/or bolts through holes which result in stress concentrations that may ultimately lead to failure. Adhesive joints, on the other hand, do not require holes and distribute the load over a larger area than mechanical joints (Choi J, & Chun Y, 2003). However, they are very sensitive to surface treatment, service temperature, humidity, and other environmental conditions (Choi JH, & Lee DG, 1996). On the other hand, for structural components that must be easily replaced or removed, mechanical fasteners play an important role. The increased use of advanced composite materials for structural applications has led to extensive research aimed at developing an understanding of the behavior of these structures to the presence of holes and inclusions. Accurate and proper design of mechanically fastened joints require the determination of the stress distribution at the contact surface and within the plate followed by the use of an appropriate failure theory to determine the strength of the joint. The method of complex functions developed by Muskhelishvili and extended to anisotropic materials by Lekhnitskii (Lekhnitskii SG., 1968) and Savin (Savin GN., 1968).

In evaluating the stress distribution in composite joints, two infinite plate solutions were superposed by de Jong to approximate the finite geometry effects of orthotropic plates. de Jong also showed the simultaneous influence of friction and load direction on the stresses in orthotropic plates with a single pinloaded hole (de Jong T., 1982). Hyer and Klang modeled the pin and its interaction with the hole by including pin-elasticity. They showed that pin-elasticity is rather unimportant in stress prediction compared to clearance, friction and elastic properties of the plate material (Hyer MW, & Klang EC., 1985). Zhang and Ueng presented a compact solution for a rigid, perfectly fitting-pin loading an infinite plate. They used a certain displacement expressions for the edge of the hole that satisfy the physical displacement requirements in conjunction with Lekhnitskii's complex functions to evaluate the stress distribution in the contact region (Zhang KD, & Ueng CES., 1984). Using the finite element analysis and a failure area index method, Ryu et al. were able to predict the failure loads of carbon/epoxy composite laminates. In their analysis, the pin-plate interface was assumed to be frictionless and the results compared with experimental data (Ryu CO, Choi JH, & Kweon JH., 2007). Lessard et al. evaluated failure of mechanically fastened joints made from AS4-3501-6 graphite epoxy laminates. They tested laminates of varying geometric ratios in order to determine failure strengths using linear and non-linear finite element models (Lessard LB, Poon C, & Fahr A., 1992). Whitworth et al. (Whitworth HA, Othieno M, & Barton O., 2003) also used finite element analysis and the Chang–Scott–Springer characteristic curve model (Chang FK, Scott RA, & Springer GS., 1983) to evaluate the stress distribution around the fastener hole in composites.

Among them, Aktas and Dirikolu (Aktas A, & Dirikolu MH., 2003) have studied the effect of stacking sequence of carbon-epoxy composite laminates, with $[0/45/45/90]_S$, and $[90/45/45/0]_S$ configuration, on pinned-joint. They found, for both configurations, that the bearing strength reaches their maximum value at W/D=4 and E/D=4 geometric configuration. Karakuzu et al. have investigated failure mode, failure load and bearing strength in a laminated woven glass-vinylester composite plate with two paralel circular holes which are subjected to traction forces by two paralel rigid pins (Karakuzu R, Taylak N, Icten B, & Aktas M., 2008). They have been observed the behavior of pin loaded composite plates with various dimensions experimentally and numerically. Sheng et al. (Sheng H, Hung C, & Chang FK., 1996) have experimentally studied the pinned-joint for various stacking sequences of a T80011/3900-2 carbon-epoxy composite laminate and determined the maximum bearing strength and the failure mode. Okutan et al. (Okutan B, Aslan Z, & Karakuzu

R., 2001) have studied the bearing strength of pin loaded Kevlar-epoxy laminates experimentally.

Numerous researchers have studied the strength of mechanically fastened joints in composite structures. Shokrieh and Lessard (Shokrieh MM, & Lessard LB., 1996) have developed a three-dimensional nonlinear finite element code to analyze the effects of material nonlinearity and edge effects on the state of stress and failure prediction near the stress concentrations of a pin-loaded graphite/epoxy laminated composite plate. Dano et al. (Dano ML, Gendron G & Piccard A., 2000) have discussed influence of failure criteria and the inclusion of geometric and shear non-linearities. Ahn et al. (Ahn HS, Kweon JH, & Choi JH., 2005) have performed a nonlinear finite element analysis to considerate the contact and friction between the pin and the laminate for unidirectional and woven composite laminated joints of an aircraft control rod. Pierron et al. (Pierron F, Cerisier F, & Grediac M., 2000) have studied the behavior of woven glass fiber epoxy pin joints both numerically and experimentally, with particular attention given to the sensitivity of the model to different parameters such as clearance, friction, and material nonlinearity.

Several authors carried out the effect of the end distance- to-diameter, and width-to-diameter ratios on the failure strength and failure mode of a mechanically fastened laminated composite plates made of carbon-epoxy, glass-epoxy, glass-vinyl ester and Kevlar-epoxy. Quinn and Matthews (Quinn WJ, & Matthews FL., 1977) have investigated the effects of stacking sequence on the pin-bearing strength in glass fiber reinforced plastic. Liu et al. (Liu D, Raju BB, & You J., 1999) have examined the thickness scaling effect on stiffness and strength of thick section composite, which is made of woven glass fabric and phenolic matrix. Wu and Hahn (Wu TJ, & Hahn HT., 1998) have investigated the bearing properties of mechanically fastened glass-fiber/vinyl-ester composite joints. The effects of geometric parameters such as edge distance, width and thickness of the specimen were evaluated and correlated with the resulting bearing strength and failure modes by the statistical method of analysis of variance.

Although Composite materials are extremely important for naval design, few researchers have been studied on the effect of sea water on composite materials. Some of them were given as follows:

Huang and Sun (Huang G, & Sun H., 2007) have investigated the effect of water immersion on the tensile strength and bending behavior of the composites experimentally. They have obtained after immersed in water at a temperature of about 30^{o} C for various periods, the composites experienced significant reduction of the tensile strength, meanwhile the bending behavior was improved.

Olmos et al. (Olmos D, Lopez-Moron R, & Gonzalez-Benito J., 2006) have studied the effect of the nature of glass fibre surface in the water absorption of glass fibres/epoxy composites. They have changed the nature of the glass fibre surfaces using three different silane coatings. Fibre, (i) 3-aminopropyltriethoxysilane, APTES; (ii) 3-aminopropylmethyldiethoxysilane, APDES and (iii) 3-aminopropyldimethylmonoethoxysilane, APMES. The presence of the silanized fibres seems to induce changes in the water absorption process of the epoxy resin decreasing the relative gain of mass at equilibrium and suggesting that the glass fibre surface may induce a change in the structure of the epoxy matrix.

Rhee et al. (Rhee KY, Lee SM, & Park SJ., 2004) have investigated compressive behavior of carbon/epoxy composite in the deep-sea environment, they have performed the compressive tests on seawaterabsorbed unidirectional ([0º]64) carbon/epoxy thick composite at various hydrostatic pressures up to 270 MPa. The results have showed that the compressive properties of seawater-absorbed carbon/epoxy composite underwent significant changes with increasing pressure. Fracture strength and fracture strain increased with pressure in a linear fashion.

Kootsookos and Mouritz (Kootsookos A, & Mouritz AP., 2004) have investigated the effect of seawater immersion on the durability of glass- and carbon- fibre reinforced polymer composites experimentally. They showed that when immersed in seawater at a temperature of 30 ºC for over two years, the composites experienced significant moisture absorption and suffered chemical degradation of the resin matrix and fibre/matrix interphase region.

The polymer matrix in almost all GRP composites for seawater applications is isophthalic polyester or vinyl ester resin (Smith CS., 1990). When used in marine applications it is essential that glass/polyester and glass/vinyl ester composites retain their mechanical properties and do not degrade when immersed in seawater for many years. A disadvantage of using polyester-based composites in seawater is that the polymer matrix and fibre/matrix interphase can be degraded by a hydrolysis reaction of unsaturated groups within the resin. Seawater degradation can cause swelling and plasticisation of the polyester matrix and debonding at the fibre/matrix interface that may reduce the mechanical properties. This problem can be alleviated by using vinyl esterbased composites that generally have superior chemical stability in seawater.

Another disadvantage of using GRP composites in marine structures is their relatively low Youngs modulus. The modulus is typically below 40 GPa because of the low stiffness of glass fibres, and this makes it difficult to build ultra-light marine structures with adequate stiffness. For this reason, marine composite structures requiring high stiffness are often built using carbon fibre composite. Carbon/epoxy laminate is occasionally used, but the high cost of epoxy resin has led to increased use of carbon/ polyester and carbon/vinyl ester composites in racing yachts, naval patrol vessels, offshore drilling components, and civil infrastructure for strengthening bridge pylons. A concern with using carbon fibre composites in marine structures is the limited understanding and small database of information of their long-term durability in seawater. Composite marine structures can be immersed continuously in seawater for 30–40 years. While a large amount of information is available on the seawater durability of glass/polyester and glass/vinyl ester composites because of their use in marine structures over many years, much less is known about the seawater durability of carbon fibre composites. The aim of this research is to compare the seawater durability, moisture absorption behaviour, degradation mechanisms and mechanical properties of glass/polyester and glass/vinyl ester composites against carbon/ polyester and carbon/vinyl ester composites. The materials studied are representative of composite materials used in ships, offshore drilling platforms and bridges. In this paper, durability is defined as the ability of a composite material to retain its original physical, chemical and mechanical properties when immersed in seawater. The composites were immersed in seawater at a temperature of 30 C, which is about the maximum water temperature off the coast of northern Australia during the summer season. The mass change is compared between the composites, and the mechanisms responsible for differences in the durability behaviour between the materials are investigated. In addition, the effect of water absorption on the fibre/resin interphase region is examined using scanning electron microscopy and mode I interlaminar fracture testing. The effect of seawater immersion on the flexural stiffness and strength of the composites is also determined.

In this study the effect of the sea water on the bearing strength behavior of the glass-epoksy laminated composite were investigated. The ratio of the edge distance to the pin diameter (E/D), and the ratio of the specimen width to the pin diameter (W/D) were systematically varied during experiments. The ratio of the edge distance to the pin diameter (E/D) were changed from 1 to 5 and the ratio of the specimen width to the pin diameter (W/D) were selected 3 and 4 for the study. The hole of the plate is subjected to a traction force by a pin. The specimens were kept in sea water for 1, 3, 6 and 9 months of immersing period.

CHAPTER TWO
COMPOSITE MATERIALS

2.1 Introduction

In the most general of terms, a composite is a material that consists of two or more constituent materials or phases. Traditional engineering materials (steel, aluminum, etc.) contain impurities that can represent different phases of the same material and fit the broad definition of a composite, but are not considered composites because the elastic modulus or strength of the impurity phase is nearly identical to that of the pure material. The definition of a composite material is flexible and can be augmented to fit specific requirements. In this text a composite material is considered to be one that contains two or more distinct constituents with significantly different macroscopic behavior and a distinct interface between each constituent (on the microscopic level). This includes the continuous fiber laminated composites of primary concern herein, as well as a variety of composites not specifically addressed (Staab, 1999).

2.2 Historical Development of Composite Materials

Composite materials have been in existence for many centuries. No record exists as to when people first started using composites. Some of the earliest records of their use date back to the Egyptians, who are credited with the introduction of plywood, papier-mâché, and the use of straw in mud for strengthening bricks. Similarly, the ancient Inca and Mayan civilizations used plant fibers to strengthen bricks and pottery. Swards and armor were plated to add strength in medieval times. An example is the Samurai Sword, which was produced by repeated folding and reshaping to form a multilayered composite (it is estimated that several million layers could have been used). Eskimos use moss to strengthen ice in forming igloos. Similarly, it is not uncommon to find horse hair in plaster for enhanced strength. The automotive industry introduced large-scale use of composites with the Chevrolet Corvette. All of these are examples of man-made composite materials. Bamboo, bone, and celery are examples of cellular composites that exist in nature. Muscle tissue is a multidirectional fibrous laminate. There are numerous other examples of both natural and man-made composite materials (Staab, 1999).

The structural materials most commonly used in design can be categorized in four primary groups: metals, polymers, composites, and ceramics. These materials have been used to various degrees since the beginning of time. Their relative importance to various societies throughout history has fluctuated. Figure 1 show a chronological variation of the relative importance of each group from 10,000 B.C. and extrapolates their importance through the year 2020 (Staab, 1999).The dramatic increase in the use of composite materials in all types of engineering structures (e.g., aerospace, automotive, and underwater structures, as well as in medical prosthetic devices, electronic circuit boards, and sports equipment) and the number of journals and research papers published in the last two decades attest to the fact that there has been a major effort to develop composite material systems, and analyze and design structural components made from composite materials (Reddy, 1997).

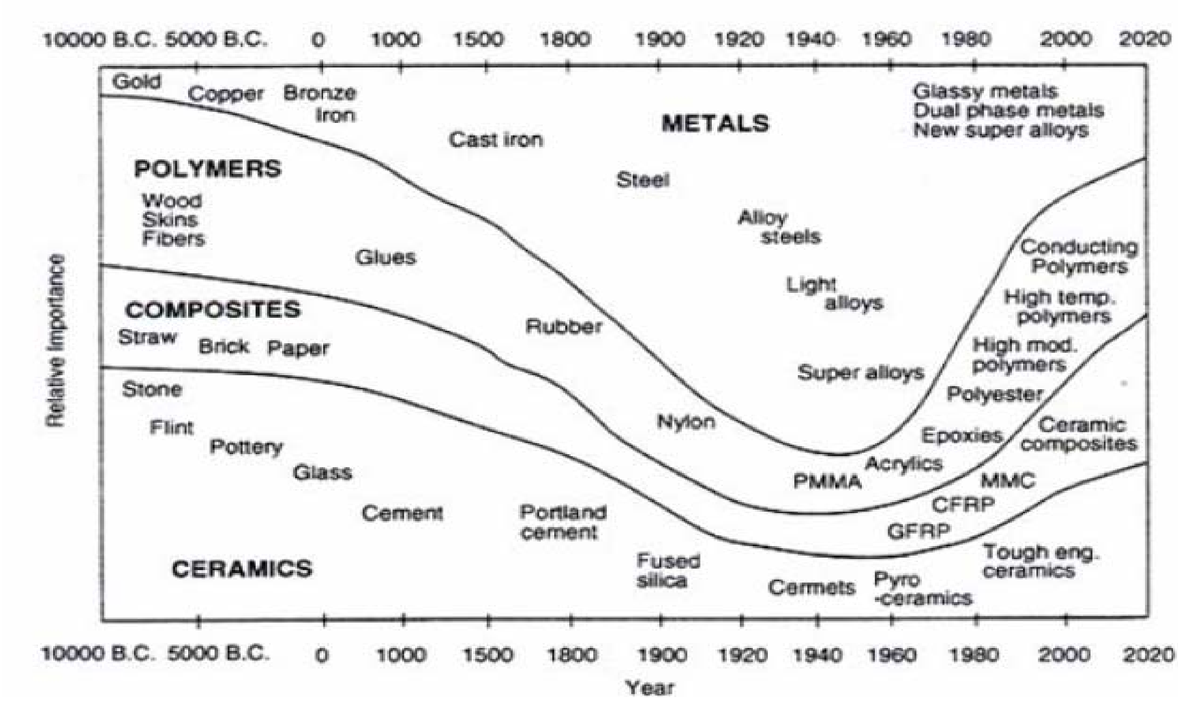

Figure 2.1 Relative importance of material development through history

2.3 Characteristics of Composite Materials

The constituents of a composite are generally arranged so that one or more discontinuous phases are embedded in a continuous phase. The discontinuous phase is termed the reinforcement and the continuous phase is the matrix. As exception to this is rubber particles suspended in a rigid rubber matrix, which produces a class of materials known as rubber-modified polymers. In general the reinforcements are much stronger and stiffer than the matrix. Both constituents are required, and each must accomplish specific tasks if the composite is to perform as intended (Staab, 1999).

A material is generally stronger and stiffer in fiber form than in bulk form. The numbers of microscopic flaws that act as fracture initiation sites in bulk materials are reduced when the material is drawn into a thinner section. In fiber form the material will typically contain very few microscopic flaws from which cracks may initiate to produce catastrophic failure. Therefore, the strength of the fiber is greater than that of the bulk material. Individual fibers are hard to control and form into useable components. Without a binder material to separate them, they can become knotted, twisted, and hard to separate. The binder (matrix) material must be continuous and surround each fiber so that they are kept distinctly separate from adjacent fibers and the entire material system is easier to handle and work with (Staab, 1999).

The physical and mechanical properties of composites are dependent on the properties, geometry, and concentration of the constituents. Increasing the volume content of reinforcements can increase the strength and stiffness of a composite to a point. If the volume content of reinforcements is too high there will not be enough matrix to keep them separate, and they can become tangled. Similarly, the geometry of individual reinforcements and their arrangement within the matrix can affect the performance of a composite. There are many factors to be considered when designing with composite materials. The type of reinforcement and matrix, the geometric arrangement and volume fraction of each constituent, the anticipated mechanical loads, the operating environment for the composite, etc., must all be taken into account (Staab, 1999). In addition, the advantage of composite materials is that, if well designed, they usually exhibit the best qualities of their components or constituents and often some qualities that neither constituent possesses. Some of the properties that can be improved by forming a composite material are strength, stiffness, corrosion resistance, wear resistance, attractiveness, weight, fatigue life, temperature-dependent behavior, thermal insulation, thermal conductivity, acoustical insulation. Naturally, not all of these properties are improved at the same time nor is there usually any requirement to do so. In fact, some of the properties are in conflict with one another, e.g., thermal insulation versus thermal conductivity. The objective is merely to create a material that has only the characteristics needed to perform the design task (Jones, 1999).

Isotropic, homogeneous materials (steel, aluminum, etc.) are assumed to be uniform throughout and to have the same elastic properties in all directions. Upon application of a uniaxial tensile load, an isotropic material deforms in a manner similar to that indicated in Figure 2 (the dashed lines represent the undeformed specimen). Assuming a unit width and thickness for the specimen, the transverse in-plane and out-of-plane displacements are the same. Unlike conventional engineering materials, a composite material is generally nonhomogeneous and does not behave as an isotropic material. Most composites behave as either anisotropic or orthotropic materials. The material properties of an anisotropic material are different in all directions. There is typically a coupling of extension and shear deformation under conditions of uniaxial tension. The response of an anisotropic material subjected to uniaxial tension is also illustrated in Figure 2. There are varying degrees of anistropic material behavior, and the actual deformation resulting from applied loads depends on the material (Staab, 1999).

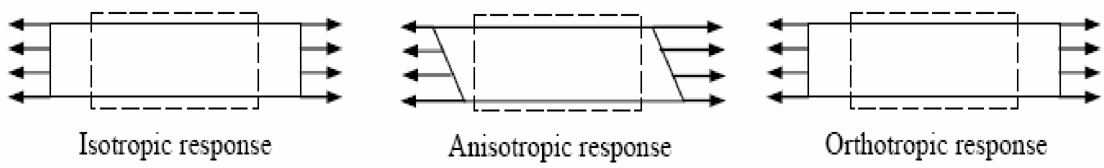

Figure 2.2 Typical material response for isotropic, anisotropic, and orthotropic materials subjected to axial tension

The material properties of an orthotropic material are different in three mutually perpendicular planes, but there is generally no shear-extension coupling as with an anisotropic material. The transverse in-plane and out-of-plane displacements are not typically same, because Poisson's ratio is different in these two directions. Figure 2 also illustrates orthotropic material response. Although it appears similar to that of an isotropic material, the magnitudes of the in-plane and out-of-plane displacements are different (Staab, 1999).

2.4 Classifications of Composite Materials

Composite materials are usually classified according to the type of reinforcement used. Two broad classes of composites are fibrous and particulate (Staab, 1999). Four commonly accepted types of composite materials are (Jones, 1999):

1. Fibrous composite materials that consist of fibers in a matrix.
2. Laminated composite materials that consist of layers of various materials.
3. Particulate composite materials that are composed of particles in a matrix.
4. Combinations of some or all of the first three types.

2.4.1 Fibrous Composite Materials

A fibrous composite consists of either continuous (long) or chopped (whiskers) fibers suspended in a matrix material. A continuous fiber is geometrically characterized as having a very high length-to-diameter ratio. Long fibers in various forms are inherently much stiffer and stronger than the same material in bulk form. A whisker is generally considered to be a short, stubby fiber. Schematics of both types of fibrous composites are shown in Figure 2.3. Naturally, fibers and whiskers are of little use unless they are bonded together to take the form of a structural element that can carry loads. The binder material is usually called a matrix (not to be confused with the mathematical concept of a matrix). Matrix materials can be polymers, metals, ceramics, or carbon (Jones, 1999; Staab, 1999).

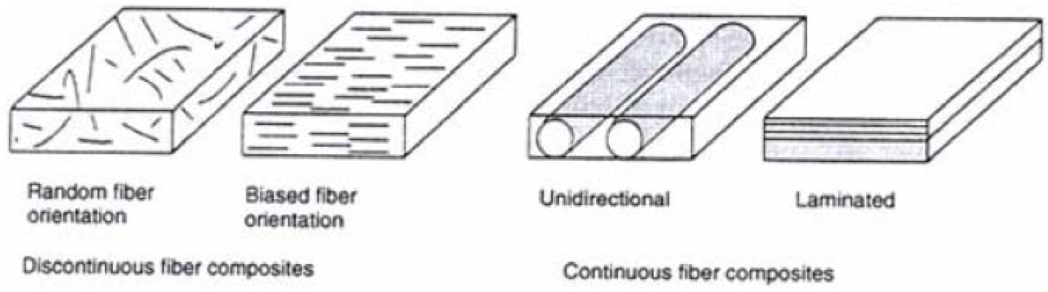

Figure 2.3 Schematic representations of fibrous composites (Staab, 1999).

2.4.2 Laminated Composite Materials

Laminated composite materials consist of layers of at least two different materials that are bonded together. Lamination is used to combine the best aspects of the constituent layers and bonding material in order to achieve a more useful material. The basic building block of a laminate is a lamina which is a flat (sometimes curved as in a shell) arrangement of unidirectional fibers or woven fibers in a matrix. Two typical flat laminas along with their principal material axes that are parallel and perpendicular to the fiber direction are shown in Figure 2.4. The matrix can be organic, metallic, ceramic, or carbon (Jones, 1999).

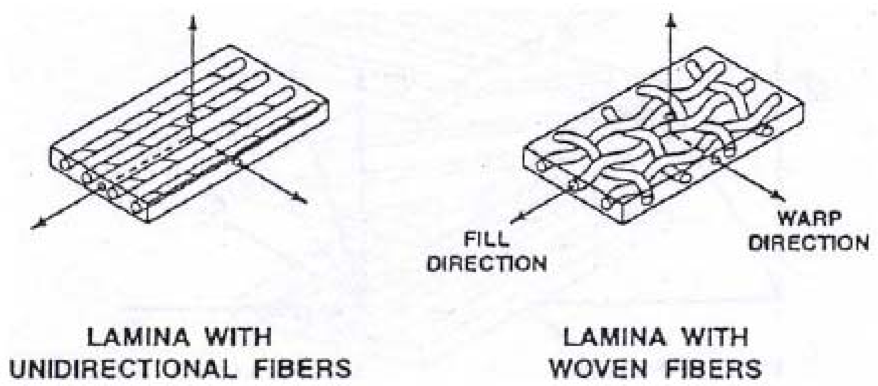

Figure 2.4 Two principal types of lamina (Jones, 1999)

A laminate is a bonded stack of lamina with various orientations of principal material directions in the lamina as in Figure 2.5. Note that the fiber orientation of the layers in Figure 2.5 is not symmetric about the middle surface of the laminate. The layers of a laminate are usually bonded together by the same matrix material that is used in the individual lamina. The mechanical response of a laminate is different from that of the individual lamina that forms it. The laminate's response depends on the properties the properties of each lamina, as well as the order in which the lamina are stacked. A major purpose of lamination is to tailor the directional dependence of strength and stiffness of a composite material to match the loading environment of the structural element. Laminates are uniquely suited to this objective because the principal material directions of each layer can be oriented according to need.

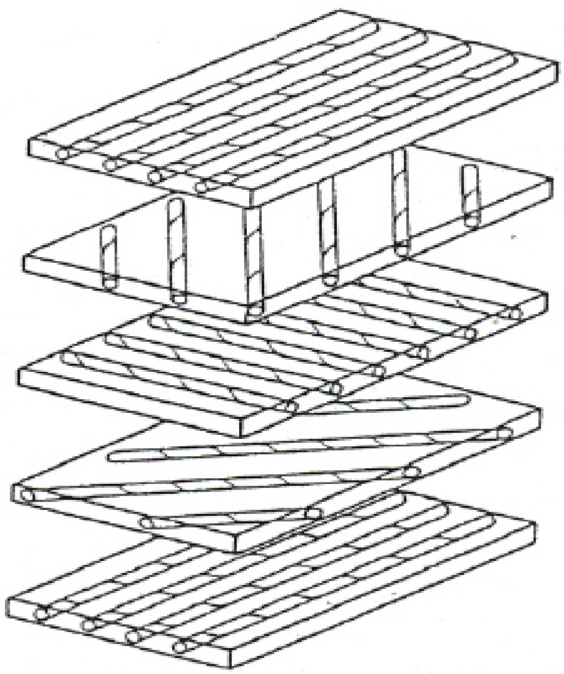

Figure 2.5 Unbonded view of laminate construction
(Jones, 1999)

2.4.3 Particulate Composite Materials

Particulate composite materials consist of particles of one or more materials suspended in a matrix of another material. The particles can be either metallic or nonmetallic as can the matrix. The four possible combinations of these constituents are described in the following paragraphs (Jones, 1999).

1. Nonmetallic particles in nonmetallic matrix composite materials.
2. Metallic particles in nonmetallic matrix composite materials.
3. Metallic particles in metallic matrix composite materials.
4. Nonmetallic particles in metallic matrix composite materials.

Particles can have virtually any shape, size or configuration. Examples well-known particulate composites are concrete and particle board. The response of a particulate composite can be either anisotropic or orthotropic. Such composites are used for many applications in which strength is not a significant component of the design. A schematic of several types of particulate composites is shown in Figure 2.6 (Staab, 1999).

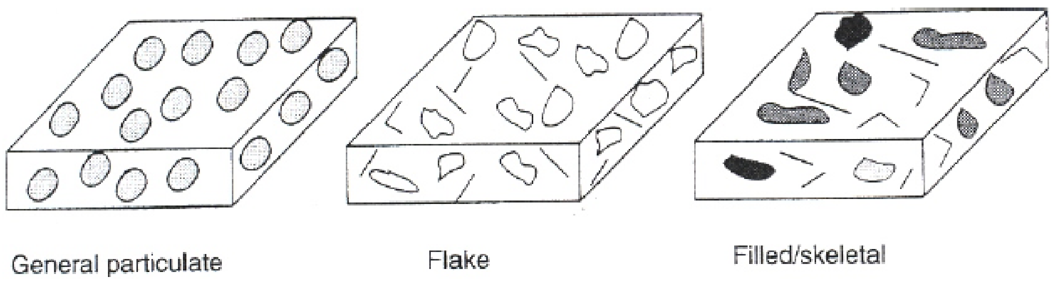

Figure 2.6 Schematic representations of particulate composites (Staab, 1999)

2.4.4 Combinations of Composite Materials

Numerous multiphase composite materials exhibit more than one characteristic of the various classes, fibrous, laminated, or particulate composite materials, just discussed. For example, reinforced concrete is both particulate (because the concrete is composed of gravel in a cement-paste binder) and fibrous (because of the steel reinforcement). Also, laminated fiber-reinforced composite materials are obviously both laminated and fibrous composite materials. Thus any classification system is arbitrary and imperfect. Laminated fiber-reinforced composite materials are a hybrid class of composite materials involving both fibrous composite materials and lamination techniques. Here, layers of fiber-reinforced material are bonded together with the fiber directions of each layer typically oriented in different directions to give different strengths and stiffness of the laminate in various directions.

2.5 Laminate Joints in Composite Structures

Composite materials are commonly used in structures that demand a high level of mechanical performance. Their high strength to weight and stiffness to weight ratios has facilitated the development of lighter structures, which often replace conventional metal structures. Due to strength and safety requirements, these applications require joining composites either to composites or to metals (Okutan & Karakuzu, 2002). High stiffness and strengths can be attained for composite laminates. However, these characteristics are quite different from those of ordinary materials to which we often need to fasten composite laminates. Often, the full strength and stiffness characteristics of the laminate can not be transferred through the joint without a significant weight penalty. Thus, the topic of joints or other fastening devices is critical to the successful use of composite materials (Jones, 1999).

The two major classes of laminate joints are bonded joints as in Figure 2.7 and bolted joints as in Figure 2.8. Often, the two classes are combined, for example, as in the bonded-bolted joint of Figure 2.9. Joints involving composite materials are often bonded because of the natural presence of resin in the composite and are often also bolted for reasons discussed later. Several characteristics of fiber-reinforced composite materials render them more susceptible to joint problems than conventional metals. These characteristics are weakness in in-plane shear, transverse tension, interlaminar shear, and bearing strength relative to the primary assets of a lamina, the strength and stiffness in the fiber direction (Jones, 1999).

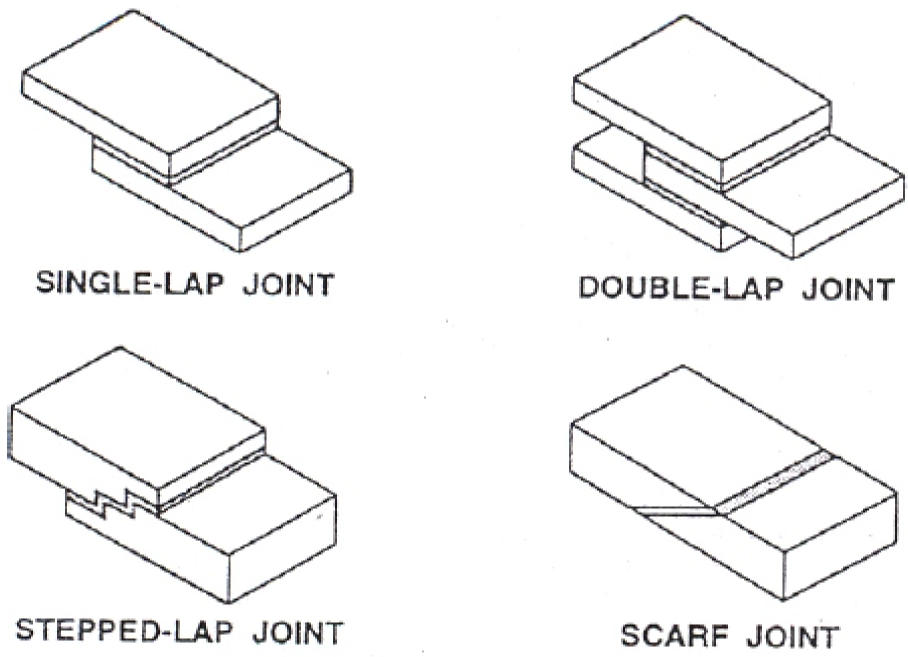

Figure 2.7 Bonded joints of composite structures

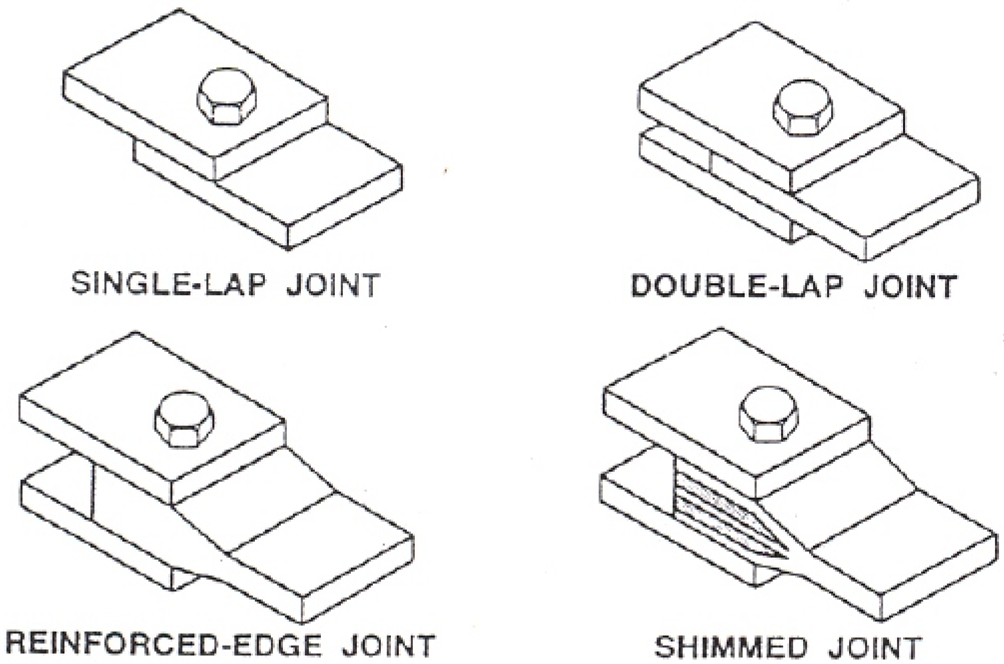

Figure 2.8 Bolted joints of composite structures

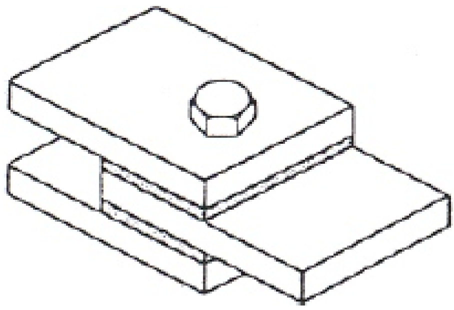

Figure 2.9 Bonded - bolted joints of composite structures

2.5.1 Bonded Joints of Composite Materials

Adhesively bonded joints have been used widely in structures as a result of advancements in adhesive technology. Adhesive bonding allows structural components with different mechanical properties to be joined, such as composite and metal components. Analytical and experimental studies have been concentrated on the stress and deformation states of the adhesive layer and adherents forming the adhesive joint (Apalak et al., 2003). The fundamental design problem in bonded joints is to get enough bond area in shear to carry the load through the joint. Bond area in tension is of little value because of the typically low strength of bonding materials compared to the far higher strength of the metals or composite materials being joined.

2.5.2 Bolted Joints of Composite Materials

Many papers deal with the failure analysis of bolted composite joints. This is mainly due to the fact that joining composite structural components often requires mechanical fasteners which ultimately makes mechanical response difficult to predict. Contrary to many metallic structural parts, for which the strength of the joints is mainly governed by the shear and the tensile strengths of the pins, composite joints present specific failure modes due to their heterogeneity and anisotropy (Pierron et al., 2000). The principal failure modes of bolted joints are (1) bearing failure of the materials as in the elongated bolt hole of Figure 2.10, (2) tension failure of the material in the reduced cross section through the bolt hole, (3) shear-out or cleavage failure of the material (actually transverse tension failure of the material), and (4) bolt failures (mainly shear failures). Of course, combinations of these failures do occur (Jones, 1999).

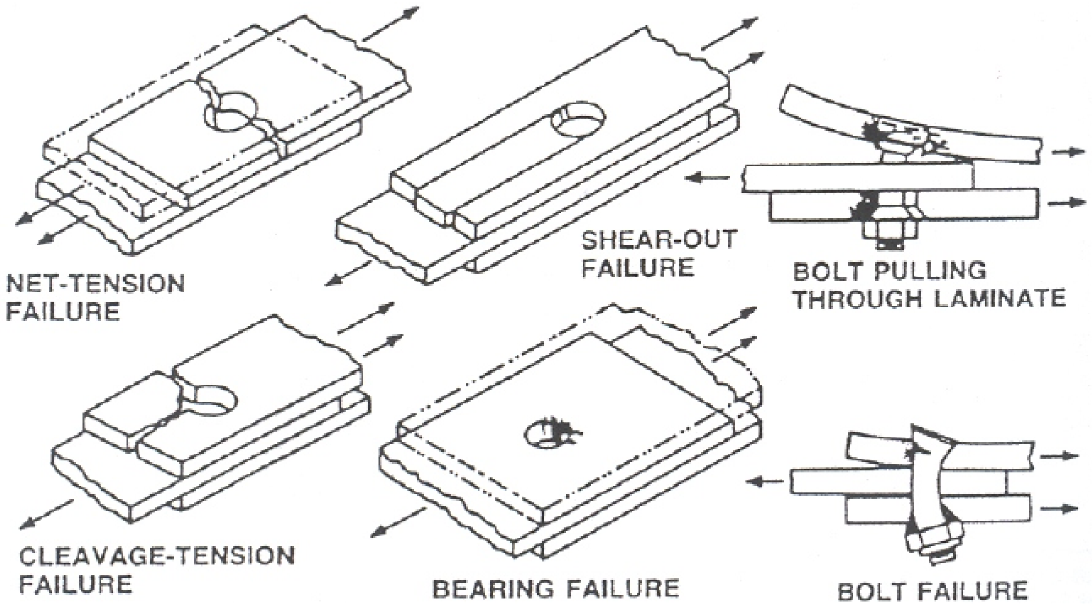

Figure 2.10 Bolted joint failures

2.5.3 Bonded-Bolted Joints of Composite Materials

Bonded-bolted joints generally have better performance than either bonded or bolted joints. The bonding results in reduction of the usual tendency of a bolted joint to shear out. The bolting decreases the likelihood of a bonded joint debonding in an interfacial shear mode. The usual mode of failure for a bonded-bolted joint is either a tension failure through a section including a fastener or an interlaminar shear failure in the composite material or a combination of both. Bonded-bolted joints have good load distribution and are generally designed so that the bolts take all the loads. Then, the bolts would take all the loads after the bond breaks (because the bolts do not receive load until the bond slips). The bond provides a change in failure mode and a sizeable margin against fatigue failure.

2.5.4 Design of Joints of Composite Materials

It is clear that joints must be considered an integral part of the design process. A structural joint represents a critical element in virtually all hardware designs. In a composite structure, the joint may be made totally or partially of composite materials. The method of joining may be adhesive bonding or mechanical fastening; in many situations the latter method is preferred because of its nonpermanent nature. The designer is confronted, in many instances, with a decision as to whether to specify a bonded or a bolted joint concept for a given structural attachment. Basic considerations that influence this decision usually include the following (Okutan, 2001):

1. The magnitude of the loading, typically expressed as a force per unit joint width that must be transmitted from one end to the other.
2. The geometrical constraints within which the load transfer must be accomplished.
3. The desired reliability of the joint.
4. Environmental factors in joint operation.
5. A need for repetitive assembly and disassembly.
6. Joint efficiency desired (the strength-weight factor).
7. Cost of manufacture, assembly, and inspection.

In addition, to estimate the strength of single pin-loaded specimens, the static strengths are defined as (Okutan, 2001):

Net-tension Strength : The stress at net-tension section, at failure, is given by

$$\left(\sigma_t\right)_{ult} = \frac{P_{ult}}{\left(W - D\right)\cdot t} \tag{2.1}$$

where P_{ult} is the failing load of the member, *W* is the joint width at net-section, *D* is the hole diameter and t the joint thickness.

Bearing Strength : The bearing strength of a composite material is expressed in the form,

$$\left(\sigma_b\right)_{ult} = \frac{P_{ult}}{D \cdot t} \tag{2.2}$$

Shearing Strength: The strength in this case is given as,

$$\left(\tau_s\right)_{ult} = \frac{P_{ult}}{2 \cdot E \cdot t} \tag{2.3}$$

where E is the distance (parallel to the load) between the hole center and the free edge, usually known as the edge distance.

The behavior of joint could be influenced by four groups of parameters (Chen et al., 1994; Okutan, 2001).

1. *Material parameters*; fiber types and form, resin type, fiber orientation, laminate, stacking sequence, etc.
2. *Geometry parameters*; specimen width (W) or ratio of width to hole diameter (W/D), edge distance (E) or ratio of the edge distance to hole diameter (E/D), specimen thickness (t), hole size (D), and pitch for multiple joints.
3. *Fastener parameters*; fastener type, fastener size, clamping area and pressure, washer size and hole size and tolerance.
4. *Design parameters*; loading type (tension, compression, fatigue, etc.), loading direction, joint type (single lap, double lap), geometry (pitch, edge distance, hole pattern etc.), environment and failure criteria.

It is clear that, in view of the very large number of variables involved, a complete characterization of joint behavior is impossible. Rather, the approach should be to determine as thoroughly as possible the behavior of basic joints and to hopefully infer the influence of the more important parameters, from which the behavior of joints and materials can be predicted (Okutan, 2001).

CHAPTER THREE
ENVIRONMENTAL EXPOSURE

3.1 Introduction

While not yet common place, polyurethane resins have become more widely used as composite matrix mamaterials in the past decade, especially for pultrusion processing. The growth in polyurethane use has been driven by the outstanding composite properties and potential for high pultrusion line speeds that have been reported using these matrices. High transverse strength, interlaminar shear strength and damage resistance exhibited by polyurethane composites create the potential for simplifying the reinforcement lay-up and reducing profile thickness.

Because they tend to perform well under such conditions, composites are used in many applications in which they are exposed to aggressive, potentially degrading environments. Therefore, evaluation of pultruded profiles in such environments is critical to ensure functionality is maintained over time. As with environmental exposure, performance of a component in real world tests of cutting, machining, drilling, bonding and mechanical assembly is important to prove viability in an application.

Polyurethane pultrusion technology is under development or has been commercialized in applications ranging from structural channels to tubes and beams to electrical components to window lineals and stiffeners to sporting goods. In each case, the pultruded profiles undergo some form of secondary operations before end use. For processes such as cutting and assembly, the toughness and durability of polyurethane composites can pay significant dividends in reduced scrap, ease of assembly, decreased labor or reduced assembly cost.

3.2 Water Absorption

Many long term performance measures are linked to a material s propensity to absorb moisture, especially for those materials that are sensitive to hydrolysis. High water absorption can result in significant swelling stresses and subsequent fiber-matrix debonding, resulting in loss of composite strength and stiffness and providing opportunity for more water ingress and hydrolytic polymer degradation.

3.3 Sea Water Immersion

In applications such as grating for off-shore oil platforms, sheet pile for sea walls and structural components for marine docks, profiles are obviously exposed to sea water. Compared to fresh or distilled water, sea water tends to be a more aggressive environment since the metal salts can catalytically promote hydrolysis. Many factors could be chosen to judge long term performance. Since these exposure tests were limited to twelve weeks duration, a sensitive material characteristic was needed to differentiate the various composites. This study focused on the change of mechanical properties and the change of bearing strength after 1, 3, 6 and 9 months sea water immersion.

General purpose competitive resins all contain ester linkages in the polymer backbone which can hydrolyze over time, decreasing resin strength. In addition to hydrolysis, the salt water can diffuse into voids in the composites potentially causing resin-fiber delamination and additional strength and stiffness reduction.

3.4 Acid Immersion

Pultruded composites are commonly used in chemical process environments and may potentially be exposed to strong acids which can degrade the matrix and potentially the reinforcement. While E-glass-based composites without a surfacing veil are not typically exposed to strong acids, such composites over their lifecycle could be exposed to acid rain or electric fields which can generate nitric acid in the presence of nitrogen, ozone and water.

CHAPTER FOUR
MEASUREMENT OF BASIC MATERIAL PROPERTIES

4.1 Introduction

The purpose of this chapter is to review briefly the most used methods for mechanical testing of composite materials and their constituents. Much of our knowledge about the special nature of composite behavior has been derived from experimental observations. The measurement of mechanical properties is also an important element of the quality control and quality assurance processes associated with the manufacture of composite materials and structures. Due to the special characteristics of composites, such as anisotropy, coupling effects and the variety of possible failure modes, it has been found that the mechanical test methods that are used for conventional metallic materials are usually not applicable to composites. Thus, the development and evaluation of new test methods for composites has been, and continues to be, a major challenge for the experimental mechanics community. The technology associated with composite test methods and test equipment has become just as sophisticated as that associated with the corresponding analytical methods. Many of these test methods have evolved into standards which have been adopted by the American Society for Testing and Materials (ASTM) (Gibson, 1994).

Nine independent elastic constants are required to define the mechanical response of an orthotropic lamina (Staab, 1999). The determination of basic material properties of unidirectional laminated composite plate under static loading conditions using experimental method has always been a key issue in the research on composite materials. With the rise of huge variety of composites, the need for an efficient and reliable way of measuring these properties has become more important. The experiments, if conducted properly, generally reveal both strengths and stiffness characteristics of the material (Okutan, 2001).

The strengths characteristics are;

X : Axial or longitudinal strength (1 direction)

Y : Transverse strength (2 direction)

S : Shear strength (1-2 plane)

The stiffness characteristics are;

E_1, E_2 : Longitudinal and transverse Young modulus

ν_{12} : Poisson's ratio

G_{12} : Shear modulus

4.2 Experimental Process

It will be considered the mechanics of materials approach in describing fiber-matrix interactions in a unidirectional lamina owing to tensile and compressive loadings. The basic assumptions in this vastly simplified approach are as follows (Mallick, 1993):

1. Fibers are uniformly distributed throughout the matrix.
2. Perfect bonding exists between fibers and matrix.
3. The matrix is free of voids.
4. Applied loads are either parallel to or normal to the fiber direction.
5. The lamina is initially in a stress-free state (i.e., no residual stresses are present)
6. Both fibers and matrix behave as linearly elastic materials.

Experiments are carried out using Instron 1114 Test Machine in Mechanics Laboratory at Dokuz Eylül University.

Figure 4.1 A view of the Instron 1114 test machine

A personal computer is also linked to this testing machine for data acquisition. Applied load and displacement are monitored for static experiments. In addition, the strain is also measured by using strain gages. The geometries and standards of the test specimen are illustrated in Table 4.1 (Gibson, 1994; Jones, 1999; Okutan, 2001).

The required basic material properties are estimated under three primary loading modes that are tension, compression and in-plane shear.

Table 4.1. Geometries of the experiment specimens

Determinable Properties	Symbol and Unit	ASTM Test Method	Specimen Geometry
Axial or longitudinal modulus	E_1 (MPa)		
Axial Poisson's ratio	ν_{12} (-)	ASTM 3039-76	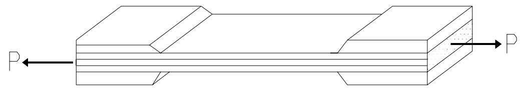
Longitudinal tensile strength	X_t (MPa)		
Transverse modulus	E_2 (MPa)		
Transverse Poisson's ratio	ν_{21} (-)	ASTM 3039-76	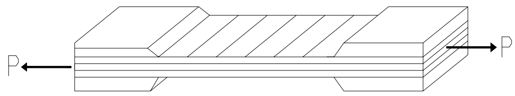
Transverse tensile strength	Y_t (MPa)		
Shear modulus	G_{12} (MPa)	ASTM D 7078	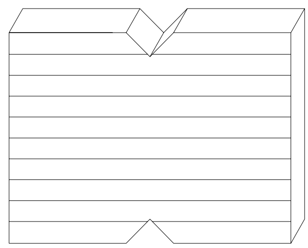
Shear Strength	S (MPa)		
Longitudinal compressive strength	X_C (MPa)	ASTM 3410-75	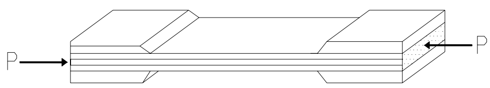
Transverse compressive strength	Y_C (MPa)	ASTM 3410-75	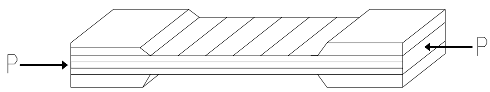

4.2.1 Measurement of the tensile properties

Tensile properties of glass-epoxy laminated composite plate such as Young's modulus (E_1), (E_2); Poisson's ratio (ν_{12}), (ν_{21}); and laminated plate longitudinal tensile strengths (X_t) and transverse tensile strength (Y_t) are measured by static tension testing longitudinal $[0^o]_{12}$ and transverse $[90^o]_{12}$ unidirectional specimens according to the ASTM D3039-76 standard test method. The tensile test specimen is straight sided and has a constant cross-section. As illustrated in figure 4.2, the tensile test geometry to find the longitudinal tensile properties consist of twelve laminas. The laminas were positioned 0^o orientation 12.7mm wide and 203mm length.

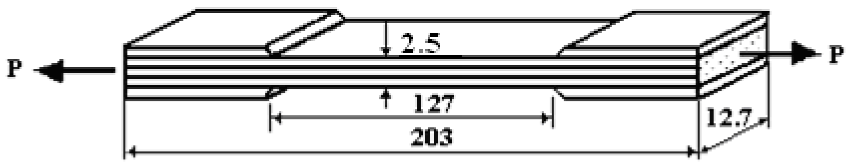

Figure 4.2 The dimensions and geometry of longitudinal tensile test specimen

The tensile specimen is positioned in the testing machine, taking care to align the longitudinal axis of the specimen and pulled at a cross-head speed of 1 mm/min. The specimens are loaded step by step up to failure under uni-axial tensile loading.

Figure 4.3 Deformed tensile test specimens to obtain longitudinal elasticity module (E_1) and poisson ratio (ν_{12})

A continuous record of load and deflection is obtained by a digital data acquisition system. Axial and transverse strains are measured by means of two-stain gauge installed in the gage section of the test specimen. The stress in the longitudinal direction is drawn as a function of longitudinal strain. The stress-strain behavior is occurred linear and final failure is occurred catastrophically. The magnitudes of E_1, ν_{12} and X_t are calculated using the tension test data and Equation (4.1).

$$\sigma_1 = \frac{P}{A} \Rightarrow E_1 = \frac{\sigma_1}{\varepsilon_1}$$

$$\nu_{12} = -\frac{\varepsilon_2}{\varepsilon_1} \qquad (4.1)$$

$$X_t = \frac{P_{ult}}{A}$$

in which A is the cross-sectional area of the specimen and perpendicular to the applied load.

Additionally, the transverse modulus E_2, minor Poisson's ratio ν_{21} and transverse tensile strength Y_t are measured from the tension test data of $[90^o]_{12}$ unidirectional laminated plate. To describe the E_2, ν_{21} and Y_t, a smooth piece of laminated plate whose principal axes perpendicular to direction of loading is taken and a strain gauge is stuck on loading direction. The test specimen for transverse tension test is prepared according to ASTM 3039-76 standards. The transverse tensile test specimen and dimensions are also illustrated in Figure 4.4.

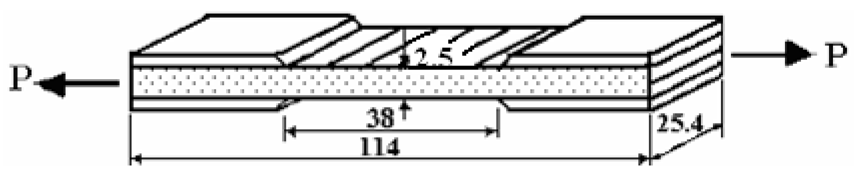

Figure 4.4 The dimensions and geometry of transverse tensile test specimen

During the measuring process, the specimen is loaded step by step up to break by a machine test and for all steps. The stress-strain behavior is occurred linear and final failure is occurred catastrophically.

Figure 4.5 Deformed tensile test Specimens to obtain transverse elasticity module (E_2) and poisson ratio (ν_{21})

The magnitudes of E_2, ν_{21} and Y_t are calculated using the tension test data and Equation (4.2).

$$\sigma_2 = \frac{P}{A} \Rightarrow E_2 = \frac{\sigma_2}{\varepsilon_2}$$

$$\nu_{21} = \nu_{12} \cdot \frac{E_2}{E_1} \quad (4.2)$$

$$Y_t = \frac{P_{ult}}{A}$$

4.2.2 Measurement of the compressive properties

Compression testing of laminated composites is one of the most difficult and interesting types of testing due to sidewise buckling of the test specimen. Many test methods have been developed and used overcome the buckling problem, incorporating variety of test specimen designs and loading fixtures. Even though an ASTM standard for compression testing has been published, there is still much discussion regarding various alternative test methods (Mallick, 1993; Gibson, 1994; Okutan, 2001).

Figure 4.6 A view of compression testing equipment

In this study, the test specimen with a very short length although unsupported gauge-length is preferred. Test specimen is unidirectional as tensile tests. Besides, it has a constant cross-section. Furthermore, the width and gauge length of test specimen is 6.4 mm and 12.7 mm, respectively as explained in ASTM 3410-75.

During the experiments, compressive load is performed $[0^o]_{12}$ and $[90^o]_{12}$ glass-epoxy laminated composite specimens.

Figure 4.7 Deformed longitudinal compressive test specimens to obtain longitudinal compressive strength (X_c)

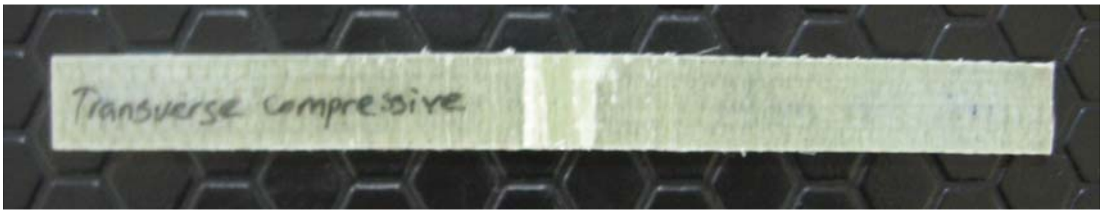

Figure 4.8 Deformed transverse compressive test specimens to obtain transverse compressive strength (Y_c)

Meanwhile, the maximum failure loads are recorded to obtain longitudinal and transverse compression strengths X_c and Y_c.

4.2.3 Measurement of the shear properties

As shown earlier, the in plane properties of a composite material are not necessarily equal to the through-thickness shear properties. Thus, test methods which will generate pure shear loading of both types are needed (Gibson, 1994). A variety of test methods have been used for measuring in-plane shear properties, such as the shear modulus G_{12} and the ultimate shear strength τ_{12} of unidirectional fiber-reinforced composites (Mallick, 1993).

It is well known that obtaining of shear properties of laminated composites is very difficult types of mechanical static tests. One of the principal difficulties in a development of shear test method for these materials is to induce a stress of pure shear in a gage section of specimen which has to be only subjected to a shear stress of a constant magnitude (Okutan, 2001). There have been many attempts to develop convenient test methods to measure the in-plane shear stress-strain response for composite materials.

The common in-plane shear test methods are;

1. ±45 Shear test
2. 10^o Off-axis test
3. Torsion tube

4. Rail shear test
5. Sandwich cross-beam test
6. T-specimen shear
7. Iosipescu shear test
8. V-Notched rail shear test

In this study, V-notched rail shear test (ASTM D 7078) was preferred for measuring the shear modulus and shear strength of composites as it combines the best features of the Iosipescu Shear (ASTM D 5379) and two-rail shear (ASTM D4255) test methods into a unified test. The 90 degree v-notch configuration of the Iosipescu shear test, and the clamped rail configuration of the two-rail shear test have been combined.

A potential problem with the standard Iosipescu shear test method when testing some materials is crushing of the edges of the specimen in the regions where it is loaded by the fixture. The two-rail shear test method utilizes loading rails clamped onto two edges of the specimen by six bolts that pass through holes in the specimen. In addition to the cost and potential specimen damage when preparing these holes, slipping of the specimen in the rails can lead to premature bearing failures as the bolts contact edges of the specimen holes, thus nullifying the test.

The ASTM D 7078 standard specimen is 76mm long (the same as the standard Iosipescu specimen), but 56mm wide (versus 20mm for the standard Iosipescu specimen), resulting in a much larger gage section (31mm wide versus 12mm). The specimen notch depth to width ratio of 0.225 is nearly the same as the 0.200 for the Iosipescu specimen, thus preserving the gage section geometry.

25mm of each end of the specimen is gripped by the fixture. That is, the specimen is gripped up to the notches, resulting in 26 of specimen being exposed between the grips.

Note in the following photograph the cutout in the lower grip assembly (shown at the left). This is to permit raising the lower grip mounted in the testing machine after the specimen has been installed in the upper grip. This cutout permits installing a specimen without having to remove the fixture from the testing machine, which is sometimes desirable, e.g., when performing elevated temperature or cryogenic tests.

Figure 4.9 V-notched rail shear test equipment

The V-notched rail shear test specimen is tested using this fixture. The strain-gauge is installed on the specimen between the notches at 45 degrees as illustrated in Figure 4.10.

Figure 4.10 V-notched rail shear test specimen before tested.

The test specimens are positioned in V-notched rail shear test fixture where the specimen is centered using the alignment pin and lightly clamped with the adjustable wedges as illustrated in Figure 4.11. Afterward the load (P) is carried out to the specimen.

Figure 4.11 V-notched rail shear test process

During the V-notched rail shear test, Instron 1114 testing machine is used for loading. The strain-gauge datas are recorded and datas are reduced to shear strains at the center of the test part and drawn as a function of the applied load. The specimen design and dimensions are illustrated in Figure 4.12.

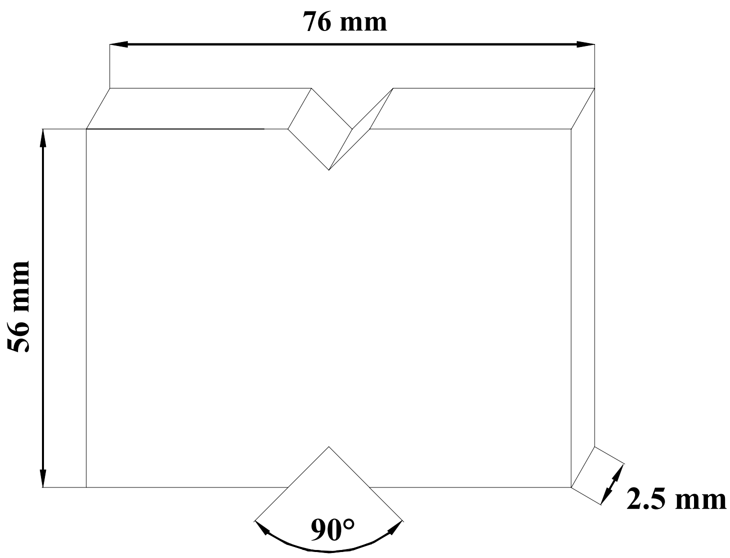

Figure 4.12 Dimensions of the V-notched rail shear test specimen

According to the V-Notched rail shear test strain-gauges connected to $[0/90]_{3S}$ orientationed specimens and shear modules were determined. The strain-gauges which pasted to specimen with 45^{o} angle were connected to the indicator with cables as illustrated Figure 4.13.

Figure 4.13 Connected indicators to the specimen in V-notched rail shear test process

Test machine was stopped by specific intervals during applying tests on different ten point. Force values were written down from computer screen and strain values were written down from indicator. An excel table were prepared by written down force and strain values.

Shear module were determined for every point by means of formules given 4.3. The main shear module were calculated by averaging detemined shear modules.

$$\tau = \frac{P}{A} = G_{12} \cdot \gamma_{12}$$

$$\gamma_{12} = 2 \cdot \varepsilon \qquad (4.3)$$

$$G_{12} = \frac{P}{2 \cdot A \cdot \varepsilon}$$

in which

P : Applied load, N

A : Specimen cross-section, mm^2

G_{12} : Shear module, GPa

γ_{12} = Shear strain

CHAPTER FIVE
EXPERIMENTAL STUDY

5.1 Introduction

Mechanical tests were performed on a pinned joints in $[0°/90°]_{3S}$ orientationed glass-fiber reinforced epoxy for a range of specimen geometry. The ratio of the edge distance to the pin diameter (E/D) was changed from 1 to 5 and the ratio of the specimen width to the pin diameter (W/D) was selected 3 and 4. Specimens were immersed sea water for 1, 3, 6 and 9 month and the effects of immersing sea water were discussed in the light of results.

5.2 Definition of the Problem Statement

Consider a composite rectangular plate of length L+E and width W with a hole of diameter D, the hole diameter (D) was fixed at a constant value of 5 mm. The hole is at a distance E, from the free edge of the plate. The geometry of problem is shown Figure 5.1. A pin is located at the center of the hole and a uniform tensile load P is applied to the plate. The load is parallel to the plate and is symmetric with respect to the centreline.

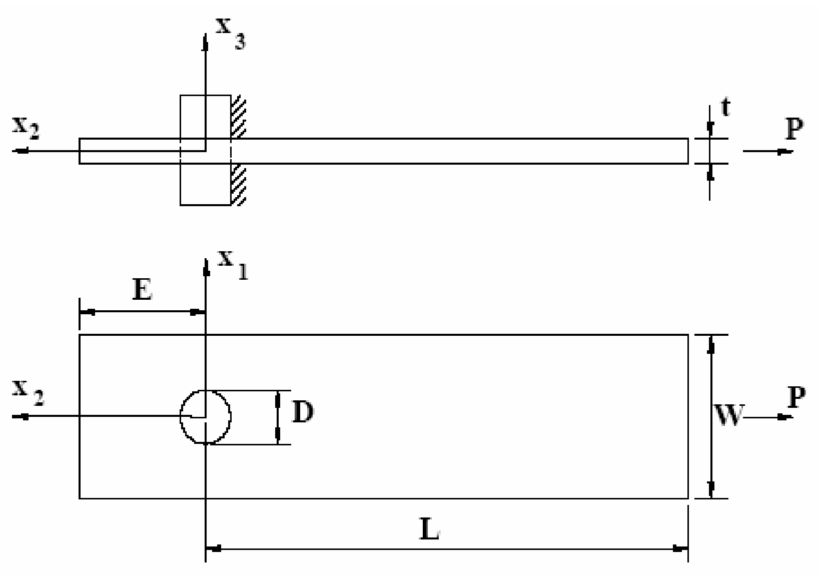

Figure 5.1. Geometry of a composite plate with a circular hole

The hole is at a distance to diameter (E/D) and width to diameter (W/D) ratios in the plate of arbitrary orientation are changed from 1 to 5 and 3 to 4, respectively.

Mechanically- fastened joints under tensile loads generally fail in three basic modes, referred to as net-tension mode, shear out mode, and bearing mode. These modes are shown in Figure 5.2. In practice combinations of these failure modes are possible.

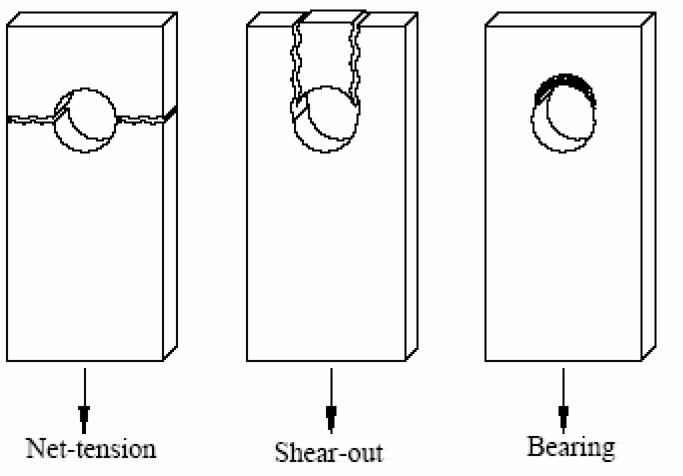

Figure 5.2 Three basic failure modes for the pinned-joint configuration

Net tension occurs catastrophically and presents the least strength. Designers are required to obtain the optimum E/D and W/D ratios to get the bearing mode, which shows the highest strength in pinned-joint uses.

5.3 Production of the Laminated Composite Plate

The laminated composite plates used in experiments were produced at Izoreel Firm in Izmir. Composite plate was consisted of twelve laminas. Thickness of each lamina was 0.3 mm. Two different lamina configurations were selected. 0^o twelve laminates for measuring the properties of composite material and $[0°/90]_{3S}$ to determine the effects of sea water on pin loaded laminated composites. All laminated plates balanced about the mid-plane both prevent thermal distortion for the period of production and to eliminate twisting and bending when under tension. All laminated composite plate were produced E-glass fiber and epoxy resin using press-mould technique. Additionally, for matrix material, epoxy CY225 and hardener HY225 were mixed in the mass ratio of 100:80. The epoxy resin and hardener mix was applied to the fibers. Then, fibers were coated with this mix. Following plies were placed one upon another as required stacking sequence. A hand roller was used to compact plies and take away entrapped air that could later lead to voids or layer separations. During the manufacturing process, the mold and lay-up were covered with a release material. Just the once the matrix material and fibers are combined, it is necessary to apply the proper temperature and pressure for specific periods of time to manufacture the fiber-reinforced laminated composite plate. Therefore, resin egnated fibers were positioned in the mold for curing. These laminas were stuck on each other by hydraulic press. The press generates the pressure and temperature required for curing. Volume fraction of the glass fiber was approximately 63 %. The mould was closed down to give the nominal thickness. The glass fiber/epoxy material was cured at 120 ^{o}C under 250 kPa pressure for 2 hours. Then the laminates were cooled to room temperature under press. Finally, laminated composite plate removed from press and cut to specimen dimensions.

5.4 Preparation of Specimens

Woven glass–fibre of twelve layer composite blanks are cut into rectangle shapes for testing through a diamond-impregnated slitting saw. All cut edges were finished using a fine silicon carbide paper to remove any edge defects. The 5mm holes, typical in size of fasteners used in many structural assemblies, were drilled using a steel drilling tool.

Specimens for each group were produced in the following manner: while keeping the W/D ratio as 3, the E/D ratio is varied as 1, 2, 3, 4 and 5; and maintaining W/D as 4, E/D is changed as 1, 2, 3, 4 and 5. After the specimens are prepared 5 groups of package prepared which made of net for dry specimens and 1, 3, 6 and 9 months sea water periods. These specimen groups were put into an aquarium which was desined before to immerse sea water. The specimens were kept into sea water 1, 3, 6 and 9 month periods. After the end of the months the specimen groups were taken out of the aquarium and then tested in the following manner.

5.5 Testing Process

The tests were conducted with reference to ASTM D953 at a room temperature of 20 ^oC. The specimens were placed in the testing machine, taking care to align the longitudinal axis of the specimen.

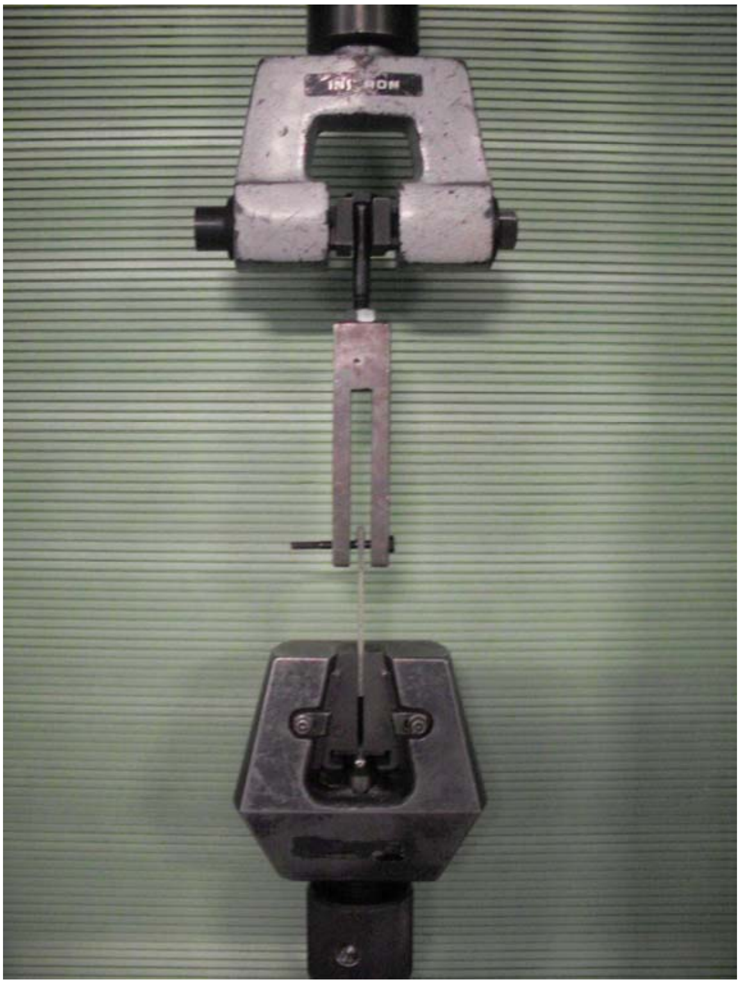

Figure 5.3 Pin loaded glass-epoksy laminated composite test process

A through-hardening steel, 42CrMo4, hardened (by heating at 850 ^oC for 2 hour and then quenched in oil at room temperature) and polished pin was later inserted in the hole without clearance. Then, experiments were performed by means of a custom fixture on the Instron 1114 Testing Machine with a speed of 1mm/min. For all geometric configurations, five specimens were tested. Mean values and standart deviations were calculted. Bearing strengths were obtained as follows,

$$\sigma_b = \frac{P_{\max}}{D \cdot t} \tag{5.1}$$

where P_{max} is the failure load, D and t denones the hole diameter and the thickness of the specimen, respectevely.

CHAPTER SIX
RESULT AND DISCUSSION

6.1 Introduction

In this chapter, a detailed discussion is given the light of experimental study results of pinned glass-epoxy laminated composite joints.

6.2 Mechanical Properties For Water Absorbed Specimens

Figure 6.1 shows longitudinal elasticity module (E_1) values are not so different from each other for unabsorbed, 1 and 3 months water absorbed conditions. When 6th month water absorbed specimens were tested we see that longitudinal elasticity module (E_1) increase. So we can say that elasticity of specmens were increased between 3-6 months.

Transverse elasticity module (E_2) values are so close to each other for unabsorbed and 1, 3, 6 months water absorbed periods. So we can say that water absorption have low effects on glass-epoksy laminated composites.

Figure 6.1 also shows that shear module (G_{12}) values decrease gradually until 6th month then shear module (G_{12}) value increases and gets greater then unabsorbed condition.

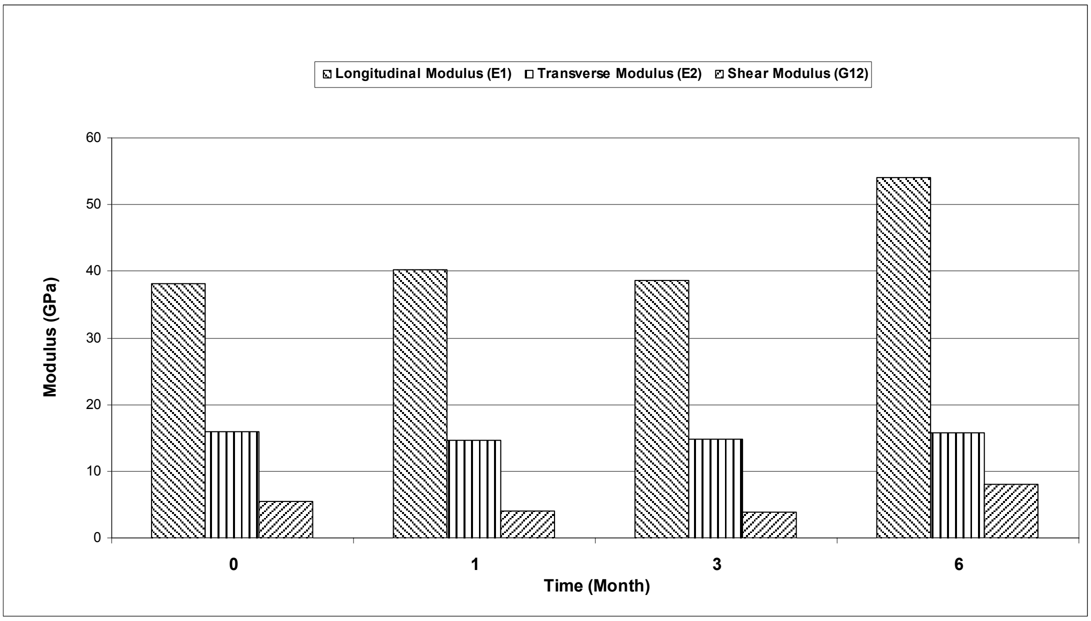

Figure 6.1 Modulus for unabsorbed and water absorbed specimens

Figure 6.2 shows the alteration of Poisson ratio (ν_{12}) for unabsorbed and water absorbed periods which include 1, 3, 6 month absorption. Poisson ratio decrease in 1st month then increase gradually for 3rd and 6th months.

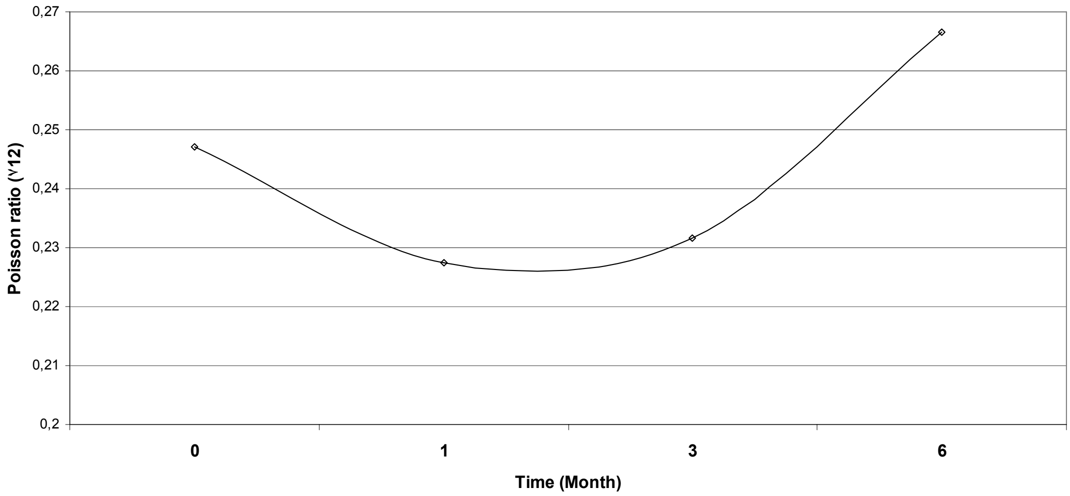

Figure 6.2 Poissons ratio for unabsorbed and water absorbed specimens

Figure 6.3 shows that longitudinal tensile strength values decreases, increases and decreases again like cosine curve.

Transverse tensile strength values are so close to each other. Therefore it is obtained that water absorption has low effects on glass-epoksy laminated composites.

Longitudinal compressive strength values increase, decrease and increase again like sine curve.

Transverse compressive strength values decrease gradually for unabsorbed and 1, 3, 6 water absorbed conditions. So it is obtained that when water absorption period getting longer transverse compressive strength values decrease.

Shear strengt values are not so different from each other so we obtain that water absorption have low effect on glass-epoksy laminated composites.

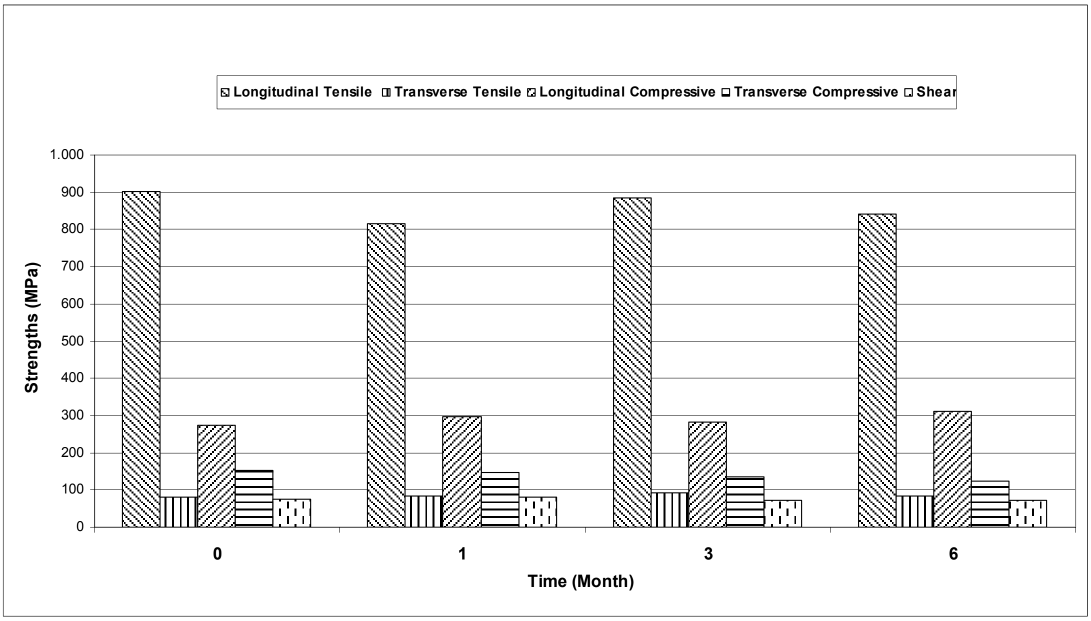

Figure 6.3 Strength values for unabsorbed water absorbed specimens

6.3 Mechanical Properties For Sea Water Immersed Specimens

Figure 6.4 shows that longitudinal elasticity module (E_1) values increases gradually till 6th month. In 6th month longitudinal elasticity module (E_1) decreases and increases again. Although longitudinal elasticity module (E_1) decreases in 6th month it is obtained that when sea water immersing period increases, longitudinal elasticity module (E_1) increases gradually. So the spcimens get more elastic.

Transverse elasticity module (E_2) values decrease, increase, decrease and increase again like cosine curve.

Shear module values decrease until 6th month then get increase to the 9th month.

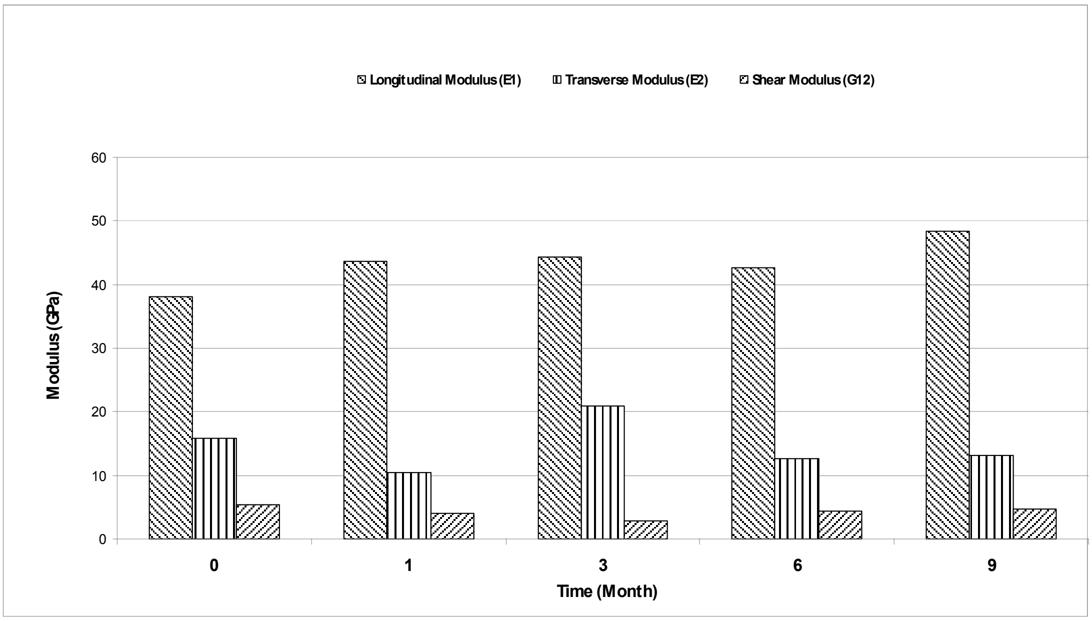

Figure 6.4 Modulus of elasticity for unimmersed and sea water immersed specimens

Figure 6.5 shows the alteration of poisson ratio (ν_{12}) for unimmersed and sea water immersed periods which include 1, 3, 6 month immersion. Poisson ratio decreases, increases, decreases and increases again like cosine curve.

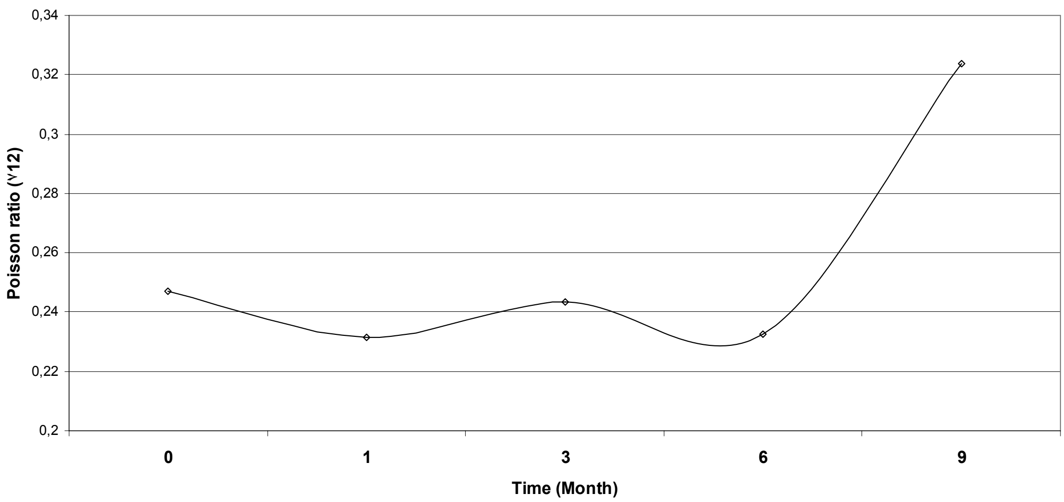

Figure 6.5 Poisson ratio values for unimmersed and sea water immersed specimens

Figure 6.6 shows lonitudinal tensile strength decrease for 1 month sea water immersing then it get increase and show low fluctuation for 3, 6 and 9 month sea water immersing period.

Transverse tensile strength show low fluctuation for unimmersed and 1, 3, 6 and 9 sea water immersing period.

Longitudinal compressive strengt values are not so different from each other so we obtain that water absorption have low effect on glass-epoksy laminated composites.

Transverse compressive strength values decrease gradually until 3rd month and get increase to 9th month for sea water immersed condition.

Shear strengt values are close to each other so it is obtained that water absorption have low effect on glass-epoksy laminated composites.

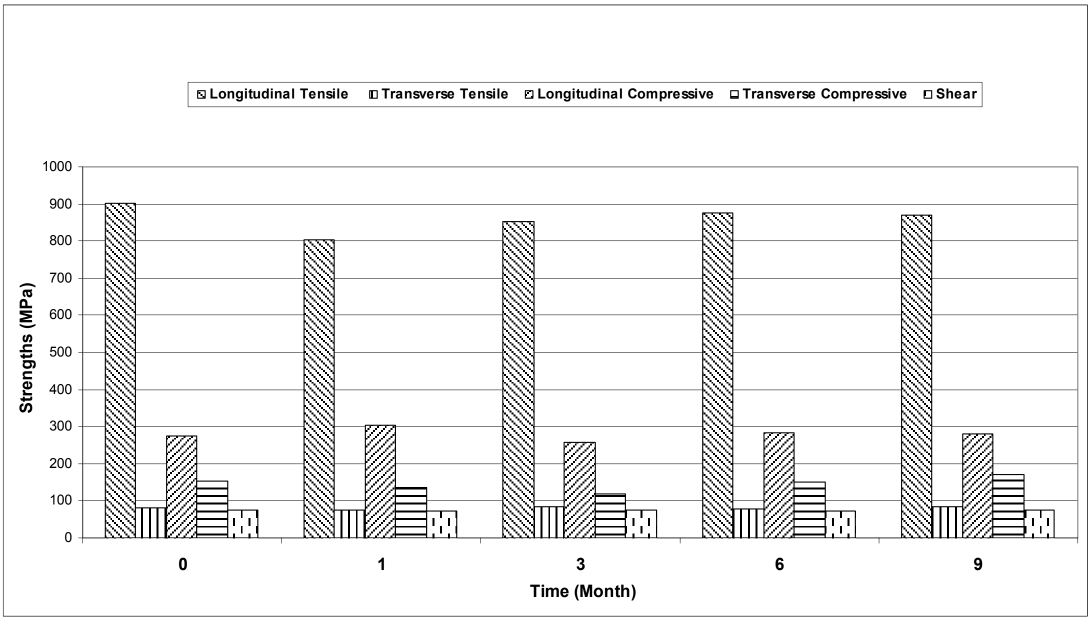

Figure 6.6 Strength values for unimmersed and sea water immersed specimens

6.4 Failure Modes

In this study there are observed three types of failure modes in pinned/bolted laminated composite plates. It is called as net-tension, shear-out and bearing failure modes. Furthermore, the mixed failure mode can be also observed in real applications.

The photographs of some tested specimens with various failure modes are illustrated in Figure 6.7 as examples of observed failure modes. The net tension failure mode is not occurred lonely because net tension mode occure when the W/D ratios are very small. The shear-out failure modes are usually observed in the outer holes, when the E/D ratios are very small and W/D ratios is equal to 3 or bigger than 3 (Figure 6.7,8-a,b). The bearing failure modes are observed for some specimens that are having big E/D and W/D ratios (Figure 6.7-c,d,e).

(a) (b) (c) (d) (e)

Figure 6.7 The photograph of some tested specimens for W/D=3 with various failure modes (9 month sea water immersed)

(a) (b) (c) (d) (e)

Figure 6.8 The photograph of some tested specimens for W/D=4 with various failure modes (9 month sea water immersed)

Meanwhile, the mixed failure modes can be observed in many tested specimens. For example, the failure mode is occurred as bearing/net-tension in inner hole whereas the bearing failure mode is only observed in the outer hole as seen in Figure 6.9.

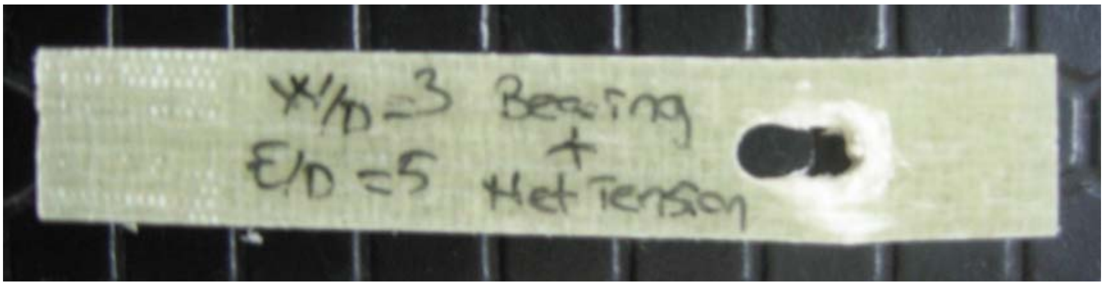

Figure 6.9 The photograph of tested specimen where occured bearing and net tension together. (3 month sea water immersed)

Bearing mode gives the highest bearing strength. Charecteristic of bearing failure mode curve is shown in Figure 6.10. As shown in force – displacement curve force increase linearly and gets maximum load then it goes on with low fluctuation under the maximum load.

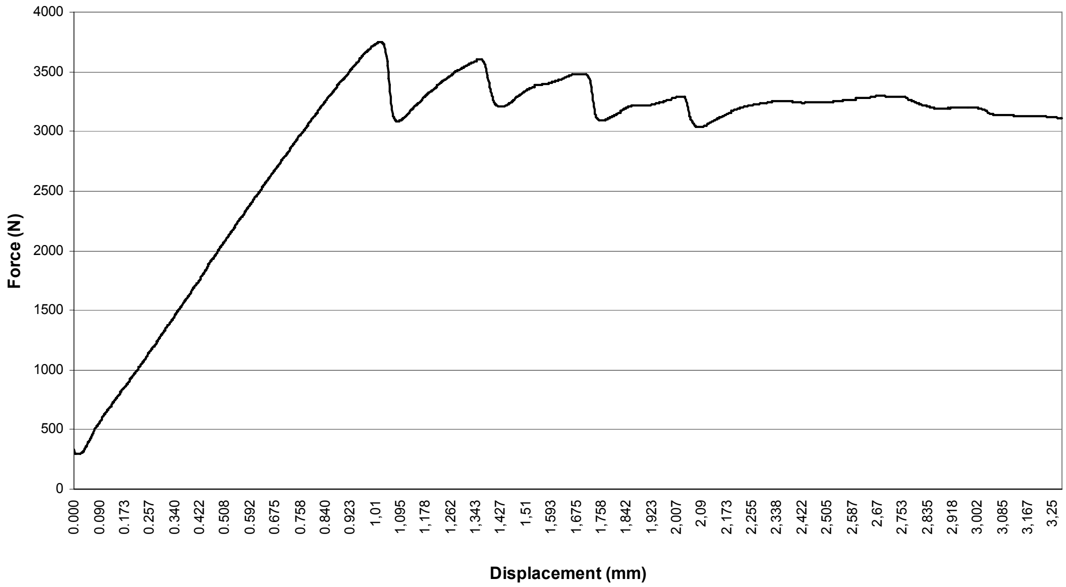

Figure 6.10 The characteristic of bearing failure mode curve of a specimen (9 month sea water immersed, W/D=3 and E/D=3)

Although net tension mode gives least strength for this study shear out mode gives least strength because of no net tension mode was seen lonely. When all specimens are investigated the failure modes of the same immersing period and configurations, same failure modes have been found with some difference. For instance, when the W/D=3 (E/D=1) the failure mode giving shear-out. Characteristic of shear-out failure mode curve is shown in Figure 6.11. As shown in force-displacement curve force increase linearly then after maximum load it get decrease gradually.

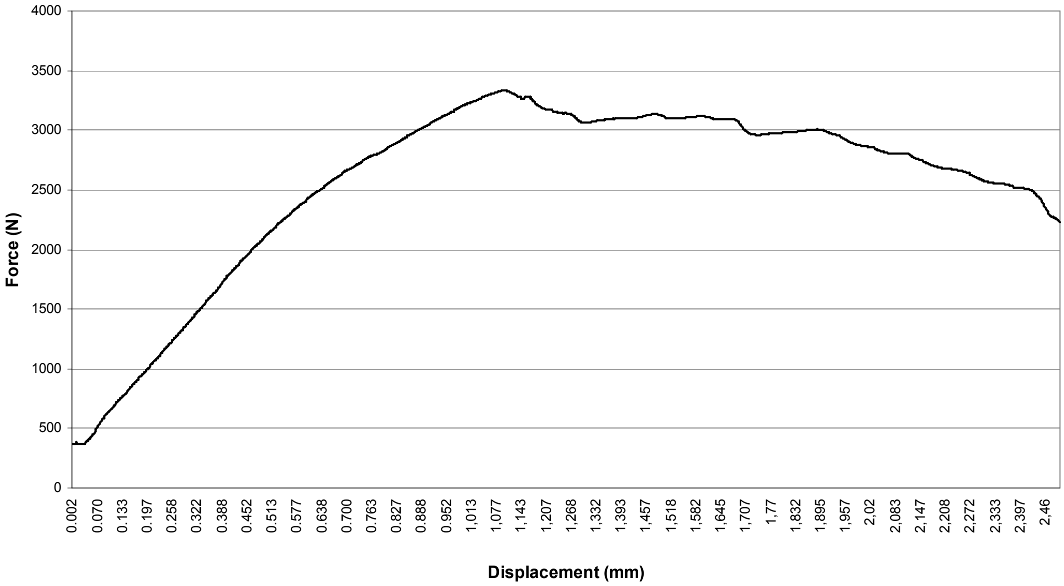

Figure 6.11 The characteristic of shear-out failure mode curve of a specimen (9 month sea water immersed, W/D=3 and E/D=2)

When W/D=3 (E/D=3, 4 and 5) the failure mode giving bearing and net-tension mixed mode together. Characteristic of bearing and net-tension mixed failure mode curve is shown in Figure 6.12. As shown in force-displacement curve force increase linearly then goes on with low fluctuation under and above maximum load and then it shows sharp decrease suddenly.

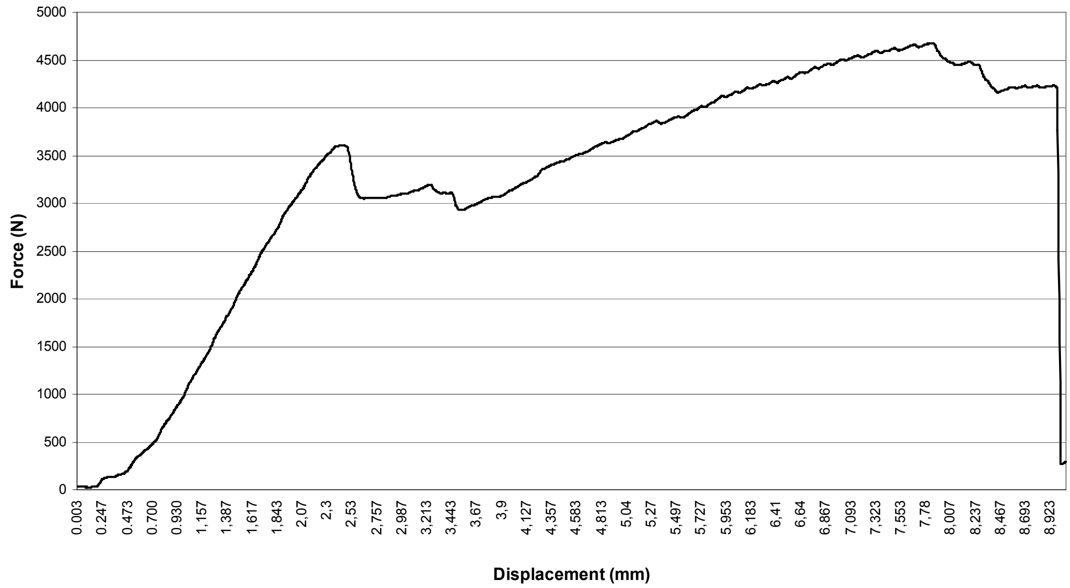

Figure 6.12 The characteristic of bearing and net-tension mixed failure mode curve of a specimen (3 month sea water immersed, W/D=3 and E/D=3)

Table 6.1 shows maximum force values, calculated avarage force values, standard deviation and damage modes for unimmersed and sea water immersed specimens. 5 specimens were tested for every E/D ratio and there were found 3 type of damage mode for W/D=3.

Table 6.2 shows maximum force values, calculated avarage force values, standard deviation and damage modes for unimmersed and sea water immersed specimens. 5 specimens were tested for every E/D ratio and there were found only 2 type of damage mode for W/D=4.

For W/D=4 the steadiest failure modes was found. For instance, when the W/D=4 (E/D=1 and 2) the failure mode giving shear-out for all the specimens for all immersing periods, W/D=4 (E/D=3, 4 and 5) the failure mode giving bearing for all the specimens for all immersing periods respectively.

B : Bearing
S : Shear-out

B+S : Bearing and Shear-out together.

Table 6.1 Maximum force values, calculated avarage force values, standard deviation and damage modes for unimmersed and sea water immersed specimens (W/D=3)

	E/D	Specimens		Time (Month) and Damage Modes									
				Unimmersed	Damage Mode	1	Damage Mode	3	Damage Mode	6	Damage Mode	9	Damage Mode
W/D=3	1	1	P (N)	1944,1250	S	1827,4375	S	1760,8813	S	1843,9113	S	1903,1400	S
		2		1661,3963	S	1425,8475	S	1532,0663	S	1375,6163	S	1549,9800	S
		3		1930,0063	S	1777,7463	S	1770,8300	S	1892,6925	S	1844,2813	S
		4		1860,3663	S	1579,9938	S	1770,8300	S	1921,9613	S	1765,8000	S
		5		1939,9538	S	1738,1963	S	1760,8813	S	1863,4238	S	1805,0400	S
		Average		1867,1700		1669,8438		1719,0975		1779,5213		1773,6488	
		Std. Deviation		119,9553		164,8924		104,6721		227,7179		134,9367	
	2	1		3581,4538	S	3059,5900	S	3312,8450	S	3014,6488	S	3335,4000	S
		2		3432,2263	S	2777,6650	S	3611,2988	S	3492,7000	S	3237,3000	S
		3		3113,8750	S	3099,1400	S	3163,6175	S	3073,1863	S	3511,9800	S
		4		3312,8475	S	3507,8288	S	3183,5150	S	3434,1638	S	3610,0800	S
		5		3133,7725	S	3505,8013	S	3511,8150	S	3785,3850	S	3727,8000	S
		Average		3314,8350		3190,0050		3356,6188		3360,0163		3484,5125	
		Std. Deviation		198,7704		314,6538		198,7953		318,4304		199,4110	
	3	1		4088,8263	B	3522,0263	B	4327,5900	B	3892,7025	B	3070,5300	B
		2		4387,2813	B	3385,1213	B	4198,2600	B	3570,7500	B	3747,4200	B
		3		4446,9713	B	3493,6313	B	4357,4350	B	3375,6263	B	3767,0400	B
		4		4635,9925	B	3553,4638	B	4068,9300	B	3619,5300	B	4188,8700	B
		5		3790,3725	B+N	3370,9238	B	4745,4263	B+N	3863,4338	B	3482,5500	B
		Average		4269,8888		3465,0338		4339,5288		3664,4088		3651,2825	
		Std. Deviation		332,3743		82,3537		254,1636		215,5866		411,5175	
	4	1		5023,9838	B	3522,0263	B	4645,9413	B+N	3190,2600	B	3198,0600	B
		2		4536,5088	B	3416,5588	B	4496,7138	B	3482,9438	B	3531,6000	B
		3		5521,4075	B	3521,0125	B	4934,4475	B+N	3609,7738	B	3855,3300	B
		4		5282,6450	B	3694,4263	B	5083,6750	B+N	3678,0675	B	4041,7200	B
		5		5471,6650	B+N	3445,9675	B	5073,7263	B	3990,2638	B	3816,0900	B
		Average		5167,2425		3519,9988		4846,9013		3590,2613		3688,5600	
		Std. Deviation		403,0421		107,9474		263,7195		291,3806		329,4028	
	5	1		5123,4688	B	3451,0388	B	4904,6025	B	3326,8463	B	3099,9600	B
		2		5402,0263	B	3378,0225	B	4775,2713	B+N	3717,0913	B	3561,0300	B
		3		5392,0775	B	3186,3538	B	4765,3238	B	3443,9200	B	3521,7900	B
		4		5511,4600	B	3228,9475	B	5163,2625	B+N	3609,7738	B	3924,0000	B
		5		5531,3563	B+N	3254,3000	B	4675,7875	B+N	3580,5050	B	3708,1800	B
		Average		5392,0775		3299,7325		4856,8500		3535,6275		3562,9925	
		Std. Deviation		162,7117		110,6258		189,7266		152,0202		303,1115	

Table 6.2 Maximum force values, calculated avarage force values, standard deviation and damage modes for unimmersed and sea water immersed specimens (W/D=4)

	E/D	Specimens		Time (Month) and Damage Modes									
				Unimmersed	Damage Mode	1	Damage Mode	3	Damage Mode	6	Damage Mode	9	Damage Mode
	1	1		2009,5938	S	1511,5413	S	1890,2113	S	2048,7913	S	1824,6600	S
		2		1840,4688	S	1419,7625	S	1641,5000	S	1902,4488	S	1834,4700	S
		3		2029,4900	S	1517,1188	S	1671,3450	S	1746,3500	S	2001,2400	S
		4		1930,0063	S	1498,8638	S	1900,1600	S	1912,2050	S	1893,3300	S
		5		1952,3900	S	1610,4175	S	1780,7788	S	1736,5938	S	1893,3300	S
		Average		1952,3900		1511,5413		1776,7988		1869,2775		1889,4063	
		Std. Deviation		74,5722		67,8080		119,9192		130,2732		70,2632	
	2	1		3501,8663	S	3274,5825	S	3432,2263	S	3160,9913	S	3394,2600	S
		2		3571,5050	S	3059,5900	S	3133,7725	S	3278,0650	S	3325,5900	S
		3		3412,3300	S	3294,8650	S	3581,4538	S	3268,3088	S	3639,5100	S
		4		3263,1025	S	3074,8013	S	3243,2050	S	3297,5775	S	3168,6300	S
		5		3233,2575	S	3235,0313	S	3402,3813	S	3639,0425	S	3453,1200	S
		Average		3396,4125		3187,7738		3358,6075		3328,7975		3396,2225	
		Std. Deviation		146,9884		112,2847		173,8281		181,3962		172,6393	
	3	1		4735,4838	B	3555,4925	B	4337,5388	B	3639,0425	B	3894,5700	B
		2		4815,0663	B	3786,7113	B	4516,6113	B	3502,4563	B	3413,8800	B
W/D=4		3	P (N)	4715,5813	B	3322,2463	B	4327,5900	B	4117,0938	B	3610,0800	B
		4		4506,6625	B	3377,0075	B	4397,2300	B	3160,9913	B	3551,2200	B
		5		4600,0138	B	3221,8488	B	4168,4138	B	3395,1388	B	3963,2400	B
		Average		4674,5613		3452,6613		4349,4763		3562,9450		3686,5975	
		Std. Deviation		121,3293		222,5812		126,1147		355,7585		233,6346	
	4	1		5876,5113	B	3478,4200	B	5232,9025	B	4000,0200	B	3521,7900	B
		2		5213,0050	B	3557,5213	B	4834,9625	B	3590,2613	B	3541,4100	B
		3		5461,7175	B	3480,4475	B	5004,0875	B	4009,7763	B	4110,3900	B
		4		5411,9750	B	3516,9563	B	5103,5713	B	3219,5288	B	3335,4000	B
		5		5203,0563	B	3355,7113	B	5063,7775	B	3414,6513	B	3472,7400	B
		Average		5433,2525		3477,8113		5047,8600		3646,8475		3596,3463	
		Std. Deviation		273,5144		75,5012		145,6359		352,1954		298,4079	
	5	1		5232,9025	B	3708,6238	B	4626,0450	B	3687,8238	B	3688,5600	B
		2		5213,0050	B	3192,4388	B	5451,7688	B	3336,6025	B	3639,5100	B
		3		5262,7475	B	3745,9638	B	5173,2113	B	3648,7988	B	3404,0700	B
		4		5640,7900	B	3491,6025	B	5362,2325	B	3814,6525	B	3433,5000	B
		5		5332,3863	B	3167,0863	B	4854,8600	B	3278,0650	B	3492,3600	B
		Average		5336,3663		3461,1425		5093,6238		3556,9388		3531,6000	
		Std. Deviation		176,0910		274,7584		347,2718		233,5775		126,2025	

Figures 6.13 and 6.14 show sea water effect on bearing strength of glass fibre composite plates pinned-joints. It can be obtained from the Figures 6.13 and 6.14 bearing strength decrease about 22.6 % gradually for all geometrical configurations, while W/D ratios change from 3 to 4 and E/D ratios change from 1 to 5. Degradation

of strength gets its maximum value while W/D ratios is change from 3 to 4 and E/D ratios change from 3 to 5. It can be obtained from the Figure 6.14 bearing strength decrease about 38 % when W/D=4 and E/D=4. When the curves were investigated separately the bearing strength gives its minimum values at E/D=1 and attains its maximum values when E/D=4.

Figures 6.13 and 6.14 show bearing trength values decrease signficantly for 1 month sea water immersion. Then bearing strength values show low fluctuation for 1, 6 and 9 month periods but in 3rd month the bearing strength values converging to the unimmersed bearing strength curve.

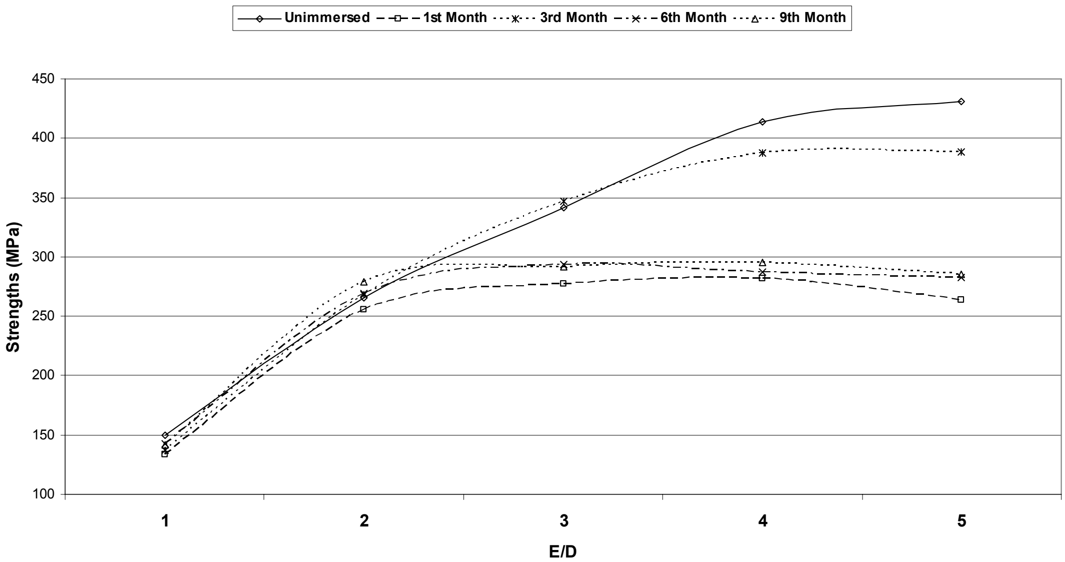

Figure 6.13 Bearing strength versus E/D ratio for sea water immersed specimens (W/D=3)

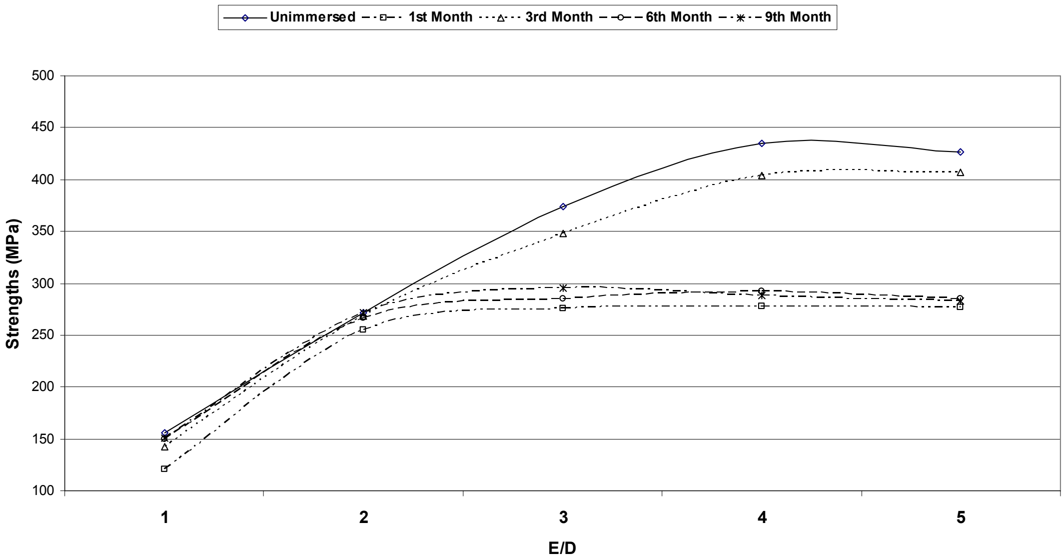

Figure 6.14 Bearing strength versus E/D ratio for sea water immersed specimens (W/D=4)

Figure 6.15 and 6.16 show bearing strengths versus time for sea water immersed specimens (W/D=3 and W/D=4)

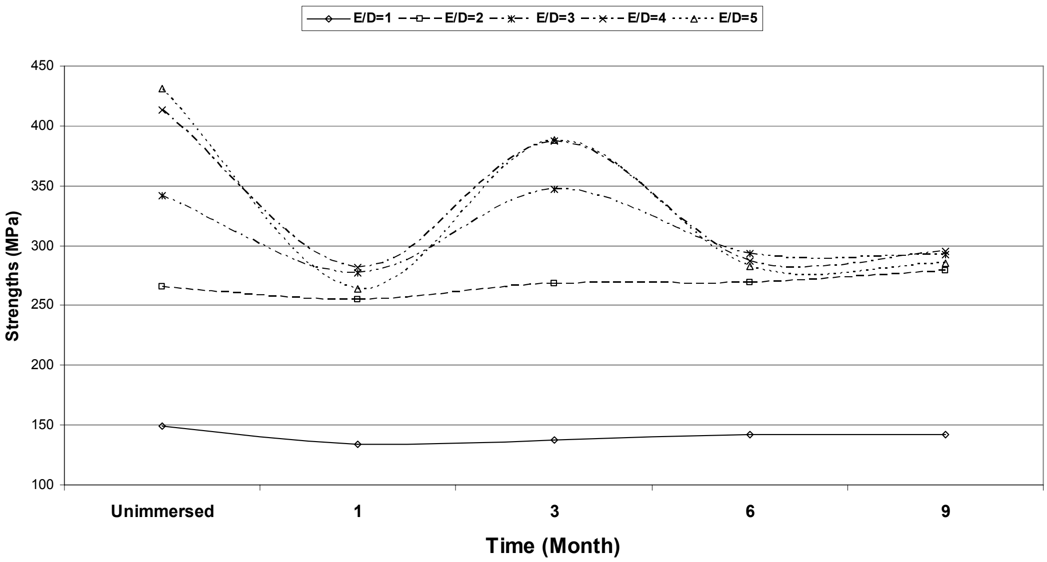

Figure 6.15 Bearing strength versus time for sea water immersed specimens (W/D=3)

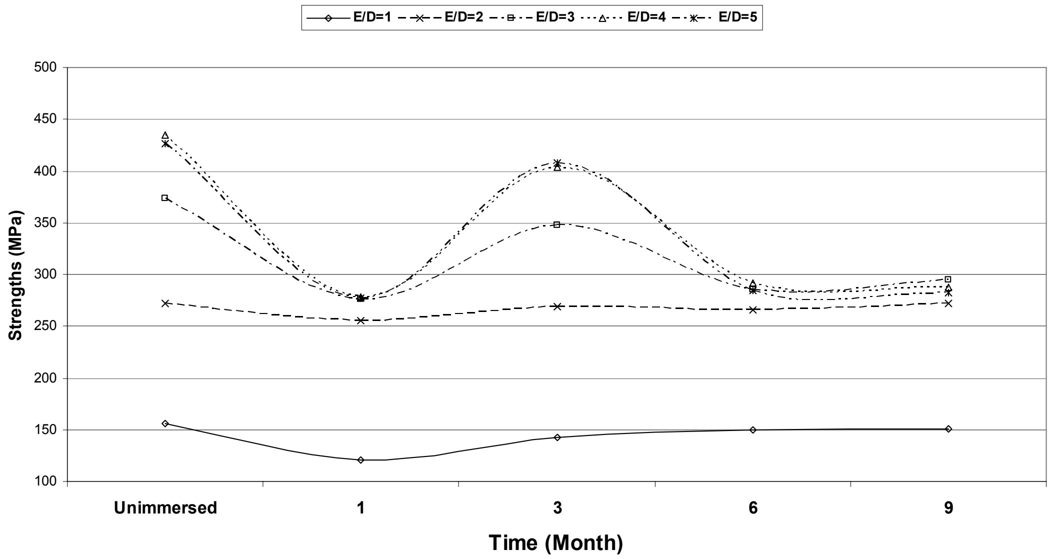

Figure 6.16 Bearing strength versus time for sea water immersed specimens (W/D=4)

When the specimens are investigated carefully, it can be also observed that the specimens immersed long period in the sea are covered with moss in some area of the specimens. Moreover, the specimens become soft with the increasing of immersing period.

CHAPTER SEVEN
CONCLUSIONS

The effect of the sea water on the bearing strength behavior of the glass epoxy composite was investigated experimentally. Specimens were cut and drilled from the composite plates. The ratios of the specimen width to the pin diameter (W/D) were changed from 3 to 4 and the ratios of the edge distance to the pin diameter (E/D) were changed from 1 to 5 with one increment. Specimens were put into an aquarium which include sea water to immerse. The specimens were kept into sea water 1, 3, 6 and 9 month periods. After that the specimens were tested and the following results were obtained.

Bearing strength decreases about 22.6 %, while W/D ratios change from 3 to 4 and E/D ratios change from 1 to 5 with 1 increment. Degradation of strength gets its maximum value while W/D ratio is equal to 4 and E/D ratio is equal to 4. When the bearing strength curves were investigated separately the bearing strength gives its maximum values when W/D=4 and E/D=4.

Failure distance of pin displacement increase with the increasing of immersing period owing to softening of the specimens.

When the W/D=3 (E/D=1 and 2) the failure mode giving shear-out W/D=3 (E/D=3, 4 and 5) the failure mode giving bearing and mixed mode respectively. For W/D=4 the steadiest failure modes was found. For instance, when the W/D=4 (E/D=1 and 2) the failure mode giving shear-out for all the specimens for all immersing periods, W/D=4 (E/D=3, 4 and 5) the failure mode giving bearing for all the specimens for all immersing periods respectively.

The specimens immersed long period in the sea are covered with moss in some area of the specimens and the specimens become soft with the increasing of immersing period.

REFERENCES

Ahn, H. S., Kweon., J. H., & Choi, J. H. (2005). Failure of unidirectional-woven composite laminated pin-loaded joints. *Journal of Reinforce Plastic Composites, 24(7),* 735–52.

Aktas, A., & Dirikolu, M. H. (2004). An experimental and numerical investigation of strength characteristics of carbon-epoxy pinned-joint plates. *Composites Science and Technology 64*, 1605–11.

Aktaş, A., & Dirikolu M. H. (2003). The effect of stacking sequence of carbon epoxy composite laminates on pinned-joint. *Composite Structures 62*, 107–11.

Aktaş, M., & Karakuzu R. (2008). Determination of Mechanical Properties of Glass-Epoxy Composites in High Temperatures. *Polymer Composites*

Aktaş, A., & Uzun I. (2008). Sea water effect on pinned-joint glass fibre composite materials. *Composite Structures, 85,* 59–63.

Apalak, M. K., Apalak, Z. G., Gunes R. & Karakas, E. S. (2003). Steady-state thermal and geometrical non-linear stress analysis of an adhesively bonded tee joint with double support. *International Journal of Adhesion and Adhesives, 23,* 115-130.

ASTM D 953-D, *Standard test method for bearing strength of plastics*, ASTM Designation. 342–6.

Chang, F. K., Scott, R. A., & Springer, G. S. (1982). Strength of mechanically fastened composite joints. *Journal of Composite Materials, 16*, 470–94.

Choi, J., & Chun, Y. (2003) Failure load prediction of mechanically fastened composite joints. *Journal of Composite Materials, 37(May)*, 2163–216.

Choi, J. H., & Lee, D. G. (1996). An experimental study of the static torque capacity of the adhesively-bonded tubular single lap joint. *The Journal of Adhesion, 55,* 245–60.

Dano, M. L., Gendron, G., & Piccard, A. (2000). Stress and failure analysis of mechanically fastened joints in composite laminates. *Composite Structures, 50*, 287–96.

De Jong, T. The influence of friction on the theoretical strength of pin-loaded holes in orthotropic plates. (1982). *Department of Aerospace Engineering, Deft University of Technology.*

Gibson, R.F. (1994). *Principals of Composite Material Mechanics.* McGraw-Hill.

Huang, G., & Sun, H. (2007). Effect of water absorption on the mechanical properties of glass/polyester composites. *Materials and Design, 28*, 1647–50.

Hyer M.W., & Klang E.C. (1985). Contact stresses in pin-loaded orthotropic plates. *International Journal of Solids and Structures, 21(9)*, 957–75.

Jones, R. M. (1999). *Mechanics of Composite Materials* (2nd ed.). US: Taylor & Francis Inc.

Karakuzu, R., Taylak, N., İcten, B., & Aktaş, M. (2008). Effects of geometric parameters on failure behavior in laminated composite plates with two parallel pin-loaded holes. *Composite Structures, 85*, 1–9.

Kootsookos A, Mouritz AP. (2004). Seawater durability of glass- and carbonpolymer composites. *Composite Science and Technology*, *64*, 1503–11.

Lekhnitskii S. G. *Anisotropic Plates*. (Ed.). (1968). English ed. (Tsai SW, Cheron T). London, Gordon and Beach.

Lessard, L. B., Poon, C., & Fahr, A. (1992). Composite pinned joint failure modes under progressive damage. *Fifth European conference on composite materials,* 49–54.

Liu, D., Raju, B.B., & You, J. (1999) Thickness effects on pinned joints for composites. *Journal of Composite Materials, 33(1)*, 2–21.

Mallick, P. K. (1993). *Fiber-reinforced composites materials, manufacturing, and design.* (2 nd ed.). New York: Marcel Decker.

Okutan, B., Aslan, Z., & Karakuzu, R. (2001). A study of the effects of various geometric parameters on the failure strength of pin-loaded woven glass-fibre reinforced epoxy laminate. *Composite Science and Technology*, 1491–7.

Okutan, B. & Karakuzu, R. (2002). The failure strength for pin-loaded multi-directional fiber-glass reinforced epoxy laminate. *Journal of Composite Materials, 36*, 2695–2712.

Olmos, D., Lopez-Moron, R., & Gonzalez-Benito, J. (2006). The nature of the glass fibre surface and its effect in the water absorption of glass fibre/epoxy composites. The use of fluorescence to obtain information at the interface. *Composite Science and Technology, 66,* 2758–68.

Pierron, F., Cerisier, F., & Grediac, M. (2000). A numerical and experimental study of woven composite pin-joints. *Journal of Composite Materials, 34(12)*, 1028–54.

Quinn, W. J., & Matthews, F. L. (1977). The effect of stacking sequence on the pinbearing strength in glass fibre reinforced plastic. *Journal of Composite Materials, 11*, 139–45.

Rhee, K. Y, Lee, S. M, & Park, S. J. (2004). Effect of hydrostatic pressure on the technical behavior of seawater-absorbed carbon/epoxy composite. *Mater Sci Eng A, 384,* 308–13.

Ryu, C. O., Choi, J. H., & Kweon, J. H. (2007). Failure load prediction of composite joints using linear analysis. *Journal of Composite Materials, 41(7)*, 865–78.

Savin G. N. *Stress concentration around holes*. (1968). New York: Pergamon Pres.

Sheng, H., Hung, C., & Chang, F. K. (1996). Bearing failure of bolted composite joints. *Journal of Composite Materials, 30*, 1285–313.

Shokrieh, M. M., & Lessard, L. B. (1996) Effects of material nonlinearity on the threedimensional stress state of pin-loaded composite laminates. *Journal of Composite Materials,30(7)*, 839–61.

Smith, C. S. (1990). *Design of Composite Structures in Composite Materials*. London and New York : Elsevier Applied Science.

Staab, G. H. (1999). *Laminar Composites* (1th ed.). US : Butterworth-Heinemann.

Whitworth, H. A., Othieno, M., & Barton, O. (2003). Failure analysis of composite pin loaded joints. *Compos Structures, 59*, 261–6.

Wu, T. J., & Hahn, H. T. (1998). The bearing strength of E-Glass/Vinyl-Ester composites fabricated by VARTM. *Composite Science and Technology, 58*, 1519–29.

Zhang, K., & Ueng, C. E. S. (1994). Stresses around a pin-loaded hole in orthotropic plates. *Journal of Composite Materials,18*, 432–46.